



Nighttime
measurements of
HO_x during the
RONOCO project

H. M. Walker et al.

Nighttime measurements of HO_x during the RONOCO project and analysis of the sources of HO₂

H. M. Walker¹, D. Stone¹, T. Ingham^{1,2}, S. Vaughan¹, B. Bandy³, M. Cain^{4,5}, R. L. Jones⁴, O. J. Kennedy⁴, M. McLeod⁴, B. Ouyang⁴, J. Pyle^{4,5}, S. Bauguitte^{6,7}, G. Forster^{8,9}, M. J. Evans^{10,11}, J. F. Hamilton¹⁰, J. R. Hopkins^{10,11}, J. D. Lee^{10,11}, A. C. Lewis^{10,11}, R. T. Lidster¹⁰, S. Punjabi^{10,11}, W. T. Morgan^{12,13}, and D. E. Heard^{1,2}

¹School of Chemistry, University of Leeds, Leeds, UK

²National Centre for Atmospheric Science, University of Leeds, Leeds, UK

³School of Environmental Sciences, University of East Anglia, Norwich, UK

⁴Department of Chemistry, University of Cambridge, Cambridge, UK

⁵National Centre for Atmospheric Science, University of Cambridge, Cambridge, UK

⁶Facility for Airborne Atmospheric Measurements (FAAM), Cranfield University, Cranfield, UK

⁷National Centre for Atmospheric Science, FAAM, Cranfield University, Cranfield, UK

⁸Centre for Ocean and Atmospheric Sciences, School of Environmental Sciences, University of East Anglia, Norwich, UK

⁹National Centre for Atmospheric Science, University of East Anglia, Norwich, UK

Title Page

Abstract

Introduction

Conclusions

References

Tables

Figures



Back

Close

Full Screen / Esc

Printer-friendly Version

Interactive Discussion



¹⁰Wolfson Atmospheric Chemistry Laboratories, Department of Chemistry, University of York, York, UK

¹¹National Centre for Atmospheric Science, University of York, York, UK

¹²School of Earth, Atmospheric and Environmental Sciences, University of Manchester, Manchester, UK

¹³National Centre for Atmospheric Science, University of Manchester, Manchester, UK

Received: 6 November 2014 – Accepted: 27 December 2014 – Published: 30 January 2015

Correspondence to: D. E. Heard (d.e.heard@leeds.ac.uk)

Published by Copernicus Publications on behalf of the European Geosciences Union.

ACPD

15, 2997–3061, 2015

**Nighttime
measurements of
HO_x during the
RONOCO project**

H. M. Walker et al.

Title Page

Abstract

Introduction

Conclusions

References

Tables

Figures



Back

Close

Full Screen / Esc

Printer-friendly Version

Interactive Discussion



Abstract

Measurements of the radical species OH and HO₂ were made using the Fluorescence Assay by Gas Expansion (FAGE) technique during a series of nighttime and daytime flights over the UK in summer 2010 and winter 2011. OH was not detected above the instrument's 1σ limit of detection during any of the nighttime flights or during the winter daytime flights, placing upper limits on [OH] of 1.8 × 10⁶ molecule cm⁻³ and 6.4 × 10⁵ molecule cm⁻³ for the summer and winter flights, respectively. HO₂ reached a maximum concentration of 3.2 × 10⁸ molecule cm⁻³ (13.6 pptv) during a nighttime flight on 20 July 2010, when the highest concentrations of NO₃ and O₃ were also recorded. Analysis of the rates of reaction of OH, O₃, and the NO₃ radical with measured alkenes indicates that the summer nighttime troposphere can be as important for the processing of VOCs as the winter daytime troposphere. Analysis of the instantaneous rate of production of HO₂ from the reactions of O₃ and NO₃ with alkenes has shown that, on average, reactions of NO₃ dominated nighttime production of HO₂ during summer, and reactions of O₃ dominated nighttime HO₂ production during winter.

1 Introduction

Trace gases emitted into the atmosphere, including pollutants and greenhouse gases, are removed primarily by oxidation. The hydroxyl radical, OH, is the most important oxidising species in the daytime troposphere, reacting with numerous species including volatile organic compounds (VOCs), CO, SO₂, and long-lived anthropogenic halogenated compounds. The oxidising capacity of the atmosphere, that is its ability to remove trace gases, is determined by the concentration of OH. During the day, primary production of OH (i.e. initialisation of the radical chain) occurs predominantly via photolysis of ozone at λ ≤ 340 nm followed by reaction of the resulting electronically excited oxygen atom, O(¹D), with water vapour. The OH-initiated oxidation of VOCs leads to the production of the hydroperoxy radical, HO₂, and together the two radicals form the

ACPD

15, 2997–3061, 2015

Nighttime measurements of HO_x during the RONOCO project

H. M. Walker et al.

Title Page

Abstract

Introduction

Conclusions

References

Tables

Figures



Back

Close

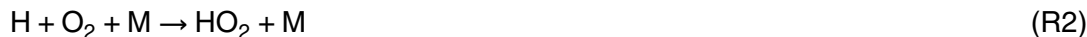
Full Screen / Esc

Printer-friendly Version

Interactive Discussion



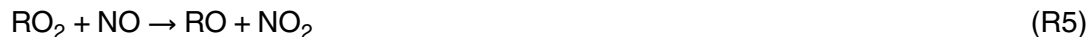
HO_x family. A key reaction in the conversion of OH to HO₂ is the reaction with CO:



Reaction of OH with VOCs results in the production of organic peroxy radicals, RO₂:



Reactions of HO₂ and RO₂ with NO propagate the HO_x radical chain, regenerating OH:



The production of OH through photolysis of ozone (and other species at longer wavelengths) is limited to daylight hours, and oxidation of trace gases at night proceeds through alternative mechanisms. Two mechanisms are known to initiate HO_x radical chemistry and oxidation chemistry at night: ozonolysis of alkenes, and reactions of the nitrate radical, NO₃, with alkenes.

Reactions of ozone with alkenes occur via addition of ozone to the double bond to form a five-membered ring called a primary ozonide. The primary ozonide decomposes to form one of two possible pairs of products, each pair consisting of a carbonyl compound and a vibrationally- and rotationally-excited carbonyl oxide termed a Criegee intermediate (CI). The simplest gas-phase CI, CH₂OO, and the alkyl-substituted CH₃CHOO, have been observed directly by photoionisation mass spectrometry (Taatjes et al., 2008, 2012, 2013; Beames et al., 2012, 2013; Welz et al., 2012; Stone et al., 2014a), by infrared absorption spectroscopy (Su et al., 2013), and by microwave spectroscopy (Nakajima and Endo, 2013, 2014). Excited CIs may be stabilised by collision with surrounding molecules (Donahue et al., 2011; Drozd and Donahue, 2011), or may undergo isomerisation or decomposition to yield products including OH, H, and subsequently HO₂ (Paulson and Orlando, 1996; Kroll et al., 2001a, b,

Nighttime
measurements of
HO_x during the
RONOCO project

H. M. Walker et al.

Title Page

Abstract

Introduction

Conclusions

References

Tables

Figures



Back

Close

Full Screen / Esc

Printer-friendly Version

Interactive Discussion



**Nighttime
measurements of
HO_x during the
RONOCO project**

H. M. Walker et al.

Title Page

Abstract

Introduction

Conclusions

References

Tables

Figures



Back

Close

Full Screen / Esc

Printer-friendly Version

Interactive Discussion



2002; Johnson and Marston, 2008). Stabilised CIs (SCIs) are known to react with a variety of compounds, including H₂O, NO₂, SO₂, and a variety of organic compounds (e.g. Mauldin III et al., 2012; Taatjes et al., 2012, 2013, 2014; Ouyang et al., 2013; Stone et al., 2014a). There is experimental evidence for the formation of OH from thermal decomposition of SCIs, on a much longer timescale than the decomposition or isomerisation of excited CIs (Kroll et al., 2001a,b). The OH produced through these ozonolysis mechanisms will proceed to oxidise other VOC species. Criegee intermediates formed in the ozonolysis of alkenes are known to be an important source of HO_x during the day and at night (Paulson and Orlando, 1996; Donahue et al., 1998; Kanaya et al., 1999; Salisbury et al., 2001; Geyer et al., 2003; Ren et al., 2003a, 2006; Heard et al., 2004; Harrison et al., 2006; Sommariva et al., 2007). The gas-phase ozonolysis of unsaturated VOCs, and in particular the role and subsequent chemistry of the Criegee intermediate, have been reviewed in detail by Johnson and Marston (2008), Donahue et al. (2011), Vereecken and Francisco (2012), and Taatjes et al. (2014).

Another key nighttime oxidant, NO₃, is formed primarily by reaction of NO₂ with ozone. NO₃ reacts with a range of species in the troposphere, and its reaction with alkenes is known to be an important nighttime oxidation mechanism (Salisbury et al., 2001; Geyer et al., 2003; Sommariva et al., 2007; Emmerson and Carslaw, 2009; Brown et al., 2011). The reaction between NO₃ and an alkene proceeds primarily via addition to a double bond, to form a nitrooxyalkyl radical, R-ONO₂. At atmospheric pressure, the main fate of the nitrooxyalkyl radical is reaction with O₂ (Berndt and Böge, 1994) to produce a nitrooxyalkyl peroxy radical, O₂-R-ONO₂. The nitrooxyalkyl peroxy radical can react with NO₂, HO₂, RO₂, NO and NO₃, of which the latter two reactions lead to formation of the nitrooxyalkoxy radical, O-R-ONO₂. The nitrooxyalkoxy radical can undergo isomerisation, decomposition, or reaction with O₂. Reaction with O₂, analogous to the reaction of organic alkoxy radicals, yields HO₂:



Thus, nighttime oxidation of hydrocarbons by NO_3 leads to production of HO_2 . Reaction of HO_2 with NO (Reaction R7), O_3 and NO_3 can generate OH :



Atkinson and Arey (2003) published a detailed review of tropospheric degradation of VOCs, including reaction with O_3 and NO_3 . A comprehensive review of nighttime radical chemistry is given by Brown and Stutz (2012).

The oxidising capacity of the nocturnal troposphere is thought to be controlled by the reactions described above, with a limited role for OH and HO_2 due to the absence of their photolytic sources. Oxidation of VOCs at night can have significant effects on daytime air quality and tropospheric ozone production (Brown et al., 2004, 2006, 2011; Wong and Stutz, 2010). Several field measurement campaigns have involved nighttime measurements of OH , HO_2 , RO_2 , and NO_3 (see Table 1), and have highlighted the importance of the vertical profile of nighttime radical concentrations and chemistry (Geyer and Stutz, 2004a, b; Stutz et al., 2004; Volkamer et al., 2010), but prior to the current work there had been no aircraft-based studies of nighttime chemistry involving measurements of both NO_3 and HO_2 , to enable vertical profiling of the lower atmosphere and full evaluation of the nocturnal radical budget. Table 1 gives details of some previous measurements and modelling of nighttime HO_x concentrations in polluted or semi-polluted environments. Highlights from these studies are discussed here, with particular attention paid to those involving measurements of HO_x , NO_3 , and O_3 , and in which the contributions made by O_3 and NO_3 to nighttime radical chemistry have been considered.

Geyer et al. (2003) report radical measurements and modelling from the 1998 Berliner Ozone Experiment (BERLIOZ). Measurements of NO_3 , RO_2 , HO_2 and OH were made by matrix isolation electron spin resonance (MIESR), chemical amplification (CA), and laser-induced fluorescence (LIF) spectroscopy at a site approximately 50 km from Berlin. HO_2 was detected at night with concentrations frequently

Nighttime measurements of HO_x during the RONOCO project

H. M. Walker et al.

Title Page

Abstract

Introduction

Conclusions

References

Tables

Figures



Back

Close

Full Screen / Esc

Printer-friendly Version

Interactive Discussion



**Nighttime
measurements of
HO_x during the
RONOCO project**

H. M. Walker et al.

Title Page

Abstract

Introduction

Conclusions

References

Tables

Figures



Back

Close

Full Screen / Esc

Printer-friendly Version

Interactive Discussion



as high as 5×10^7 molecule cm^{-3} (approximately 2 pptv), and an average concentration of 1×10^8 molecule cm^{-3} over one hour (02:00 to 03:00) of nocturnal measurements during an intensive period of the study (Holland et al., 2003). OH was usually below the limit of detection of the LIF instrument (3.5×10^5 molecule cm^{-3}). Modelling revealed that nitrate radical reactions with terpenes were responsible for producing 53 % of HO₂ and 36 % of OH radicals in the night, with ozonolysis accounting for production of the remaining 47 % of HO₂ and 64 % of OH radicals. A positive linear correlation between RO₂ and NO₃ was observed and was reproduced by the model.

Reactions of O₃ with alkenes were found to be responsible for the majority of formation of OH during the winter PUMA (Pollution of the Urban Midlands Atmosphere) campaign (a low photolysis urban environment) (Heard et al., 2004; Emmerson et al., 2005; Harrison et al., 2006). Measurements of OH, HO₂ and RO₂ were unavailable at night, but model-predicted values of these radicals were used to calculate that 90 % of nighttime initiation via HO₂ was from O₃ reactions. Without measurements of NO₃ during the campaign, there was no estimate of its contribution to radical initiation.

Modelling results from the MCMA-2003 (Mexico City) field campaign (Volkamer et al., 2010) indicate that nighttime radical production at roof-top level (approximately 16 m above the ground) was dominated by ozonolysis of alkenes, and that reactions of NO₃ with alkenes played only a minor role. The measurement site was located in a polluted urban environment, with high levels of NO, NO₂ and O₃. NO₃ was observed at a maximum concentration of 50 pptv during the night at a mean height above the ground of 70 m. Roof-top level concentrations of NO₃ were estimated using a linear scaling factor calculated from the observed O₃ vertical gradient, and were found to be, on average, 3 times lower than the concentrations measured at 70 m. This predicted vertical gradient accounts for the relative unimportance of NO₃ reactions in radical initiation at roof-top level. Propagation of RO₂ radicals to HO₂ and OH, by reaction with NO₃, was found to be negligible.

The 2006 Texas Air Quality Study (TexAQS) involved a series of nighttime flights onboard the NOAA P-3 aircraft over Houston, Texas, and along the Gulf Coast (Brown

**Nighttime
measurements of
HO_x during the
RONOCO project**

H. M. Walker et al.

Title Page

Abstract

Introduction

Conclusions

References

Tables

Figures

◀

▶

◀

▶

Back

Close

Full Screen / Esc

Printer-friendly Version

Interactive Discussion



et al., 2011). Loss rates and budgets of NO₃ and highly reactive VOCs were calculated, but there were no measurements of OH, HO₂ and RO₂ during the flights. Budgets for NO₃ show that it was lost primarily through reactions with unsaturated VOCs, but the contribution to NO₃ loss through reaction with peroxy radicals was uncertain because of the lack of direct measurements of RO₂ during the flights. NO₃ dominated VOC oxidation, being 3 to 5 times more important than O₃.

In summary, NO₃ and O₃ have both been found to dominate radical initiation in the nighttime troposphere, and in some situations the two mechanisms were found to be equally important. The relative importance of O₃- and NO₃-initiated oxidation depends on the availability of NO₃, which is determined by the amount of NO_x present in the atmosphere and the ratio of NO to NO₂, and the concentration and species distribution of VOCs (Bey et al., 2001; Geyer et al., 2003). A modelling study by Bey et al. (2001) suggests that nocturnal radical initiation is driven by alkene ozonolysis in urban environments or in environments with low NO_x concentrations, while both O₃ and NO₃ contribute to radical initiation in rural environments with moderate NO_x levels. It is expected that NO₃ dominates nocturnal radical initiation in air masses containing sufficient NO₂ and O₃ for NO₃ production while being deprived of NO (e.g. air masses downwind of urban areas). Geyer and Stutz (2004b) have found that the effects of suppressed mixing in the nocturnal boundary layer can also control whether NO₃ or O₃ dominates nighttime radical chemistry.

In this paper we report airborne measurements of OH and HO₂ made during the RONOCO (ROle of Nighttime chemistry in controlling the Oxidising Capacity of the atmosphere) and SeptEx (September Experiment) projects in 2010 and 2011. The rates of reaction between O₃, NO₃, and OH with the alkenes measured during the flights are investigated. Analysis of radical production from the nighttime reactions of O₃ and NO₃ with alkenes is also given. Comparisons are made between the daytime and nighttime chemistry studied, and between the summer and winter measurement periods. Details and results of a box modelling study, and comparison to the observations, are given by Stone et al. (2014b).

**Nighttime
measurements of
HO_x during the
RONOCO project**

H. M. Walker et al.

Title Page

Abstract

Introduction

Conclusions

References

Tables

Figures



Back

Close

Full Screen / Esc

Printer-friendly Version

Interactive Discussion



shown in Fig. 5. The flight involved a profile descent from 3350 to 460 m down the Norfolk coast and a missed approach at Southend Airport (51.6° N, 0.70° E). Plumes from European continental outflow (see Fig. 6) were intersected by a series of runs at altitudes between 460 m and the upper boundary of the polluted layer.

Flight B537 is an unusual flight within the RONOCO dataset, with high concentrations of CO, O₃, NO₃, and high temperatures compared to the values measured during other nighttime flights (see Table 3). The ambient aerosol surface area was significantly higher during B537 (nearly 800 μm² cm⁻³) than during other flights (between 100 and 400 μm² cm⁻³), and the organic aerosol concentration was significantly enhanced (Morgan et al., 2014). Footprint maps for flight B537, indicating regions where the sampled air was in contact with the surface prior to the flight, are shown in Fig. 6. The air sampled during the flight originated primarily over northern France, Belgium and Germany.

A region of high surface pressure was positioned over the UK on the 20 July, with a mean air pressure of 1012.6 hPa over the 24 h prior to the flight. The mean air temperature 24 h prior to the flight (22:00 19 July 2010 to 22:00 20 July 2010), measured at a number of Met Office weather stations in Greater London, was 22.6 °C, and reached a maximum value of 28.6 °C. Wind speeds prior to the flight were low, with an average value of 4.7 kn (2.4 ms⁻¹). No rainfall was recorded at any of the Greater London weather stations during the 24 h prior to the flight. 12.4 h of sunshine were recorded on the 20 July at Heathrow Airport (51.5° N, 0.45° W). High temperatures, combined with low wind speed, exposure to solar radiation, and little precipitation promote the formation of ozone as a result of photochemical processing of VOCs emitted at the surface (e.g. Lee et al., 2006), and offer an explanation for the high ozone mixing ratios measured during flight B537. Peak surface daytime ozone concentrations measured in Teddington, London, on 20 July were on the order of 2.0 × 10¹² molecule cm⁻³ (~ 78 ppbv) (data available at www.airquality.co.uk). Similar levels were recorded at a number of locations within Greater London.

Nighttime measurements of HO_x during the RONOCO project

H. M. Walker et al.

Title Page

Abstract

Introduction

Conclusions

References

Tables

Figures

◀

▶

◀

▶

Back

Close

Full Screen / Esc

Printer-friendly Version

Interactive Discussion



Figure 7 shows a time series of altitude, HO₂, O₃, and NO₃ mixing ratios during the flight, demonstrating very similar behaviour between the two radical species. During the missed approach at Southend Airport the mixing ratios of HO₂ and NO₃ increased with decreasing altitude, to reach values of 4.5 and 35 pptv, respectively, at 50 m above the ground. The maximum HO₂ and NO₃ mixing ratios were measured over the North Sea east of Ipswich (52.16° N, 2.34° E) at an altitude of 509 m, in the outflow of the London plume. Figure 8 shows scatter plots of HO₂ against NO₃ and O₃ during flight B537 and during the other nighttime flights during RONOCO. Strong positive correlation is evident between HO₂ and NO₃ during B537 ($r = 0.97$), while during the remaining night flights there is still a significant, though weaker, correlation ($r = 0.58$). Moderate negative correlation is evident between HO₂ and O₃ during B537 ($r = -0.46$), with weak positive correlation existing for the other nighttime flights ($r = 0.19$). The data suggest that NO₃ was an important initiator of HO_x radicals during flight B537, and that O₃ played a limited role overall during the nighttime flights. Further investigation of the roles of NO₃ and O₃ in alkene oxidation and radical initiation at night is described in Sect. 5.

5 Oxidation of alkenes and production of HO₂: method of analysis

Following the work of Salisbury et al. (2001), the total rates of reaction, Φ , of O₃ and NO₃ with the alkenes measured during RONOCO and SeptEx have been calculated:

$$\Phi_{\text{O}_3} = \sum_i^{\text{alkene}} k_{\text{O}_3+\text{alk}_i} [\text{O}_3][\text{alkene}_i] \quad (3)$$

$$\Phi_{\text{NO}_3} = \sum_i^{\text{alkene}} k_{\text{NO}_3+\text{alk}_i} [\text{NO}_3][\text{alkene}_i] \quad (4)$$

The reactions of O₃ and NO₃ with alkenes yield OH, HO₂, and RO₂ radicals. Consideration of the reaction mechanisms of NO₃ and O₃ enables calculation of the rate of

instantaneous production of HO₂ (P_{HO_2}) from the reactions of NO₃ and O₃ with the alkenes measured during RONOCO, using the chemistry scheme, rate constants and branching ratios in the MCM (Jenkin et al., 1997; Saunders et al., 2003).

Figure 9 shows a generalized reaction scheme for the reaction of NO₃ with an alkene.

The reaction between NO₃ and an alkene proceeds via addition of NO₃ to the double bond to form a nitrooxyalkyl radical, followed by rapid reaction with oxygen to yield a nitrooxyalkyl peroxy radical, RO₂ (shown as a single step in Fig. 9). The RO₂ radical can react with a number of species, of which NO, NO₃ and RO₂ lead to production of an alkoxy radical (RO). Radical termination occurs via reaction of RO₂ with HO₂ to yield a peroxide (ROOH) or with RO₂ to yield carbonyl (RC(O)CH₃) and alcohol (RCH₂OH) products. Reaction of RO with oxygen proceeds via abstraction of a hydrogen atom to yield HO₂ or an aldehyde (RCHO). This generalised scheme can be applied to the reactions of NO₃ with all the alkenes measured. The rate of instantaneous production of HO₂ is found by first calculating the fraction of RO₂ that reacts to produce RO (F_{RO}), and the fraction of RO that reacts to produce HO₂ (F_{HO_2}):

$$F_{\text{RO}} = \frac{k_3[\text{NO}] + k_4[\text{NO}_3] + 0.6k_5[\text{RO}_2]}{k_2[\text{HO}_2] + k_3[\text{NO}] + k_4[\text{NO}_3] + k_5[\text{RO}_2]} \quad (5)$$

$$F_{\text{HO}_2} = \frac{k_6[\text{O}_2]}{k_7 + k_6[\text{O}_2]} \quad (6)$$

where RO₂ represents all peroxy radicals. F_{HO_2} varies between 0 and 1 for the alkenes studied. Overall, the rate of production of HO₂ (P_{HO_2}) from reactions of NO₃ with alkenes is then given by:

$$P_{\text{HO}_2} = k_i[\text{NO}_3][\text{alkene}_i] \times F_{\text{RO}} \times F_{\text{HO}_2} \quad (7)$$

The reaction scheme for the reaction of O₃ with alkenes is more complicated because the number and type of radicals produced in the O₃ + alkene reaction depends on the structure of the alkene. The simplest case is the reaction of ozone with ethene.

Nighttime measurements of HO_x during the RONOCO project

H. M. Walker et al.

Title Page

Abstract

Introduction

Conclusions

References

Tables

Figures

◀

▶

◀

▶

Back

Close

Full Screen / Esc

Printer-friendly Version

Interactive Discussion



Nighttime measurements of HO_x during the RONOCO project

H. M. Walker et al.

Title Page

Abstract

Introduction

Conclusions

References

Tables

Figures



Back

Close

Full Screen / Esc

Printer-friendly Version

Interactive Discussion



N₂O₅. At night in summer, Φ_{NO_3} was greater than Φ_{O_3} by a factor of 2.4, but in winter Φ_{O_3} was a factor of 1.6 greater than Φ_{NO_3} . Figure 11 illustrates the importance of the butene isomers (within the VOCs measured) in the reactions of O₃ and NO₃, and therefore radical initiation and propagation. Reactions with *iso*-butene dominated NO₃ reactivity in summer (42%) and winter (53%), with *trans*-2-butene also contributing significantly (28% in summer and 32% in winter). Reactions of O₃ were dominated by *trans*-2-butene (42% in summer and 34% in winter) and propene (26% in summer and 38% in winter). The importance of these alkenes is attributed to their relatively high abundances compared to the other alkenes measured, during both summer and winter, combined with their fast rates of reaction with O₃ and NO₃.

For comparison with the reactions of O₃ and NO₃, the total rate of reaction of measured alkenes with OH has been calculated using upper limits on OH concentrations of 1.8×10^6 and 6.4×10^5 molecule cm⁻³ for the summer and winter flights, respectively, based on the FAGE instrument's limit of detection. The high upper limits make the total rate of reaction of OH with alkenes, Φ_{OH} , unrealistically high for both summer (1.6×10^5 molecule cm⁻³ s⁻¹) and winter (7.8×10^4 molecule cm⁻³ s⁻¹). However, the OH reactivity will likely be considerably lower than the values calculated using the OH upper limits. A box model constrained to concentrations of long-lived species measured during the flights (Stone et al., 2014b) predicts a mean OH concentration of 2.4×10^4 molecule cm⁻³, significantly lower than the upper limits given by the instrument's limit of detection. Using the mean modelled value for OH gives $\Phi_{\text{OH}} = 2.1 \times 10^3$ molecule cm⁻³ s⁻¹ for summer, and $\Phi_{\text{OH}} = 2.9 \times 10^3$ molecule cm⁻³ s⁻¹ for winter, indicating a diminished role for OH in alkene oxidation at night in agreement with previous studies (e.g. Geyer et al., 2003; Emmerson et al., 2005).

6.2 Daytime oxidation of alkenes

Figure 12 shows histograms of rates of reaction of O₃ and OH with alkenes during SeptEx, and O₃ and NO₃ with alkenes during winter RONOCO flights, for daytime data

**Nighttime
measurements of
HO_x during the
RONOCO project**

H. M. Walker et al.

Title Page

Abstract

Introduction

Conclusions

References

Tables

Figures

◀

▶

◀

▶

Back

Close

Full Screen / Esc

Printer-friendly Version

Interactive Discussion

only. OH was detected above the limit of detection (1.2×10^6 molecule cm^{-3}) during the SeptEx flights, so the FAGE OH data were included in the calculations, using a reaction scheme analogous to the one shown in Fig. 9. NO₃ was not detected during the day in SeptEx. NO₃ is not expected to be present at measurable concentrations during daylight hours due to photolysis, but a mean concentration of 8.3×10^7 molecule cm^{-3} (3.3 pptv) was measured during the day in the winter RONOCO flights. These measurements of low mixing ratios of NO₃ may be partly caused by interference from other daytime species as observed by Brown et al. (2005), or by the variability of the instrument baseline, which can be on the order of 1–2 pptv during vertical profiles on the aircraft (Kennedy et al., 2011). This variability is small compared to the range of NO₃ values typically observed during RONOCO flights (0–50 pptv during summer; 0–10 pptv during winter). During SeptEx, Φ_{OH} exceeded Φ_{O_3} by a factor of 8. Ethene and propene were the two most abundant alkenes measured during SeptEx and contributed significantly to OH reactivity. O₃ reactivity with alkenes was dominated by propene and *trans*-2-butene (6th most abundant alkene measured during SeptEx). NO₃ reactivity with alkenes was dominated by *trans*-2-butene and isobutene (3rd most abundant alkene measured during winter daytime flights). The total rate of reaction of O₃ and OH with alkenes during daytime SeptEx flights (3.7×10^5 molecule $\text{cm}^{-3} \text{s}^{-1}$) exceeded the total rate of reaction of O₃ and NO₃ during daytime winter RONOCO flights (6.6×10^4 molecule $\text{cm}^{-3} \text{s}^{-1}$) by a factor of 6, and was more than double the total rate of reaction of O₃ and NO₃ with alkenes during nighttime summer flights (1.4×10^5 molecule $\text{cm}^{-3} \text{s}^{-1}$). In winter daytime flights, Φ_{O_3} was greater than Φ_{NO_3} by a factor of 2.4.

Figures 11b and 12b reveal that reactions of O₃ dominated alkene reactivity during both daytime and nighttime winter RONOCO flights. The concentrations of alkenes were generally higher at night, with the total alkene concentration (sum of concentrations of alkenes measured) being 2.1×10^9 molecule cm^{-3} in the day, and 3.4×10^9 molecule cm^{-3} at night. The total measured alkene reactivity ($\Phi_{\text{O}_3} + \Phi_{\text{NO}_3}$) was

marginally higher during the day, by a factor of 1.04. This difference is attributable mainly to the change in Φ_{O_3} .

Comparison of Figs. 11a and 12b reveals that the total measured alkene reactivity ($\Phi_{\text{O}_3} + \Phi_{\text{NO}_3}$) was higher during the summer nighttime flights ($1.4 \times 10^5 \text{ molecule cm}^{-3} \text{ s}^{-1}$) than during the winter daytime flights ($6.6 \times 10^4 \text{ molecule cm}^{-3} \text{ s}^{-1}$), indicating a low oxidising environment during winter daytime. The additional contribution to measured alkene reactivity from reactions with OH has been calculated using the OH upper limits as described in Sect. 6.1. Even with this additional, upper limit OH reactivity ($1.6 \times 10^5 \text{ molecule cm}^{-3} \text{ s}^{-1}$ and $1.1 \times 10^5 \text{ molecule cm}^{-3} \text{ s}^{-1}$ for summer nighttime and winter daytime, respectively) the total summer nighttime alkene reactivity remains higher than that during winter daytime, confirming the importance of the summer nocturnal troposphere for the oxidation of the measured alkenes.

6.3 Nighttime production of HO_2 from reactions of O_3 and NO_3 with alkenes

Table 6 gives total rates ($\sum P_{\text{HO}_2}$) of instantaneous production of HO_2 from the reactions of O_3 and NO_3 with alkenes. NO_3 was not detected during the dawn summer RONOCO flights and there were no daytime RONOCO flights during summer. NO_3 dominated HO_2 production during dusk and night (68%), in agreement with Geyer et al. (2003) who found that NO_3 was responsible for 53 % of HO_2 production at night in the BERLIOZ campaign. During winter, O_3 dominated HO_2 production at all times, with a nighttime contribution of 70 %. This is in agreement with the results from the winter PMTACS-NY 2004 field campaign (Ren et al., 2006).

The total rate of instantaneous production of HO_2 at night was 3.3 times greater in summer than in winter, with production from O_3 decreasing by a factor of 1.5, and production from NO_3 decreasing by a factor of 7.8, between summer and winter. The mean temperature difference between summer and winter of 9 K is thought to be responsible for the lower NO_3 concentrations in winter ($2.0 \times 10^8 \text{ molecule cm}^{-3}$, 8.2 pptv,

Nighttime measurements of HO_x during the RONOCO project

H. M. Walker et al.

Title Page

Abstract

Introduction

Conclusions

References

Tables

Figures



Back

Close

Full Screen / Esc

Printer-friendly Version

Interactive Discussion



Nighttime measurements of HO_x during the RONOCO project

H. M. Walker et al.

Title Page

Abstract

Introduction

Conclusions

References

Tables

Figures



Back

Close

Full Screen / Esc

Printer-friendly Version

Interactive Discussion



compared to 5.8×10^8 molecule cm^{-3} , 24.5 pptv in summer), owing to the increased thermal stability of N_2O_5 , and for the reduced rate of temperature-dependent reactions between NO_3 and alkenes, and subsequent reactions. There was very little difference between summer and winter mean O_3 mixing concentrations (9.6×10^{11} molecule cm^{-3} , 39.6 ppbv, and 9.4×10^{11} molecule cm^{-3} , 38.6 ppbv, respectively).

Production of HO_2 via reactions of NO_3 and O_3 with alkenes is now examined in more detail. The rate of production from individual alkenes was calculated, and plotted in a histogram, as shown in Fig. 13 for the summer and winter nighttime data. During both summer and winter, reactions of O_3 and NO_3 with *trans*-2-butene were important sources of HO_2 , contributing on average 62 % to O_3 -initiated HO_2 production and 36 % to NO_3 -initiated production during the summer and winter flights. Reactions of NO_3 with isoprene were important during summer, contributing 28 % to NO_3 -initiated production. The importance of *trans*-2-butene, despite its relatively low abundance during summer and winter nighttime RONOCO flights (1.8 and 1.7 pptv, respectively, compared to ethene mixing ratios of 55.0 and 104.5 pptv), is attributed to its fast rates of reaction with both O_3 and NO_3 compared to the other alkenes measured. The importance of the isoprene + NO_3 reactions during the summer RONOCO flights is similarly attributed to its fast rate of reaction with NO_3 compared to the other alkenes measured. In addition there is no aldehyde-forming channel from the isoprene-derived RO radical (k_7 in Fig. 9), so that the yield of HO_2 from RO is equal to 1. The reaction of isobutene with NO_3 can proceed via one of two channels to produce two different RO_2 radicals but only one channel, with a branching ratio of 0.2, produces HO_2 . Isobutene is therefore not a dominant contributor to HO_2 production, despite being the single largest contributor to NO_3 reactivity during daytime and nighttime RONOCO flights (Figs. 11 and 12). Figure 13 highlights the small change in total production from O_3 between summer and winter, and the dramatic change in total production from NO_3 between summer and winter.

Reactions of formaldehyde with NO_3 were included in the analysis where formaldehyde data were available (mean $\text{HCHO} = 955$ pptv). The $\text{NO}_3 + \text{HCHO}$ reaction con-

Nighttime measurements of HO_x during the RONOCO project

H. M. Walker et al.

Title Page

Abstract

Introduction

Conclusions

References

Tables

Figures



Back

Close

Full Screen / Esc

Printer-friendly Version

Interactive Discussion



of NO₃ with unsaturated VOCs (80 %), with a much smaller contribution (18 %) from alkene ozonolysis. Modelled HO₂ loss is dominated by its reactions with NO₃ (45 %) and O₃ (27 %), both of which are radical propagating routes, and which are the dominant routes to OH production in the model. In fact NO₃ was found to control both radical initiation and propagation in the model.

These results are in general agreement with the results of the analysis presented in Sect. 6.1, though the model predicts a more important role for NO₃ (80 % of RO_x radical production) than is predicted by the analysis based on the observations alone (69 % of HO₂ radical production during summer), and predicts a relatively small role for O₃ in radical initiation (18 % of RO_x radical production compared to a minimum value of 31 % calculated using the observations). The model is constrained to measured values of O₃, but overpredicts NO₃. The mean measured NO₃ nighttime mixing ratio was 24.5 pptv in the summer and 8.2 pptv in the winter. The mean modelled summer and winter values are 37.4 and 20.7 pptv, respectively. This discrepancy between modelled and measured NO₃ helps to explain the model overprediction of the role of NO₃ in HO_x radical initiation during the RONOCO flights. Modelled NO₃ reactivity was dominated by *iso*-butene (36 %) and *trans*-2-butene (27 %), and modelled O₃ reactivity was dominated by *trans*-2-butene (51 %), in agreement with the nighttime alkene reactivities presented in Sect. 6.1.

Improvement to the model predictions of NO₃, N₂O₅ and HO₂^{*} was made by increasing the concentration of unsaturated VOCs in the model. Increasing the total observed alkene concentration by 4 times resulted in a modelled to observed ratio of 1.0 for HO₂^{*} and of ~ 1.2 for NO₃ and N₂O₅. Two-dimensional gas chromatography (GC × GC) analysis of the whole air samples taken during RONOCO has revealed a large number of VOCs extra to those routinely measured (Lidster et al., 2014). Calibration standards for the majority of these species are not yet available, and so quantification of their concentrations is not possible, but their detection confirms that the model overprediction of NO₃ and underprediction of HO₂^{*} are attributable to reactions of NO₃ with unquantified unsaturated hydrocarbons.

Nighttime measurements of HO_x during the RONOCO project

H. M. Walker et al.

Title Page

Abstract

Introduction

Conclusions

References

Tables

Figures



Back

Close

Full Screen / Esc

Printer-friendly Version

Interactive Discussion



The presence of unquantified unsaturated VOCs during the RONOCO campaign, suggested by the model and confirmed by the two-dimensional GC analysis, has implications for the conclusions drawn from the analysis based on the observations. The relative contributions of NO₃ and O₃ to nighttime radical initiation will change with the composition of unsaturated VOCs in the sampled air, due to the different rates of reaction of NO₃ and O₃ with different VOC species, and the rates of production of HO₂ following these reactions. The model results indicate that reaction of NO₃ with the unquantified VOCs leads to increased production of HO₂. The role of NO₃ in nighttime radical production would therefore be enhanced by the inclusion of the unquantified VOCs in the observational analysis.

8 Conclusions and future work

Nighttime radical chemistry has been studied as part of the RONOCO and SeptEx campaigns onboard the BAe-146 research aircraft during summer 2010 and winter 2011. NO₃, N₂O₅, OH and HO₂ were measured simultaneously for the first time from an aircraft, with OH and HO₂ being measured by the University of Leeds aircraft FAGE instrument. OH was detected above the limit of detection during the daytime SeptEx flights only, with a mean concentration of 1.8×10^6 molecule cm⁻³. Upper limits of 1.8×10^6 molecule cm⁻³ and 6.4×10^5 molecule cm⁻³ are placed on mean OH concentrations for the summer and winter RONOCO (night, dawn, and dusk) measurement campaigns, respectively. HO₂ was detected above the limit of detection during the summer and winter RONOCO flights and during SeptEx, with a maximum mixing ratio of 13.6 pptv measured during nighttime flight B537 on 20 July 2010. Mean nighttime HO₂ mixing ratios were significantly higher in summer than in winter. Significant concentrations (up to 176.9 pptv) of NO₃ were measured during nighttime flights, since the air masses sampled were sufficiently removed from the surface that the loss of NO₃ by reaction with NO was minimised. The RONOCO flights were therefore an excellent opportunity to study the role of NO₃ in nocturnal oxidation and radical initiation.

Nighttime measurements of HO_x during the RONOCO project

H. M. Walker et al.

Title Page

Abstract

Introduction

Conclusions

References

Tables

Figures



Back

Close

Full Screen / Esc

Printer-friendly Version

Interactive Discussion



The rates of reaction of O₃ and NO₃ with the alkenes measured have been calculated. At night during summer, NO₃ dominated alkene reactivity. Several previous nighttime studies have also found NO₃ to be the dominant nocturnal oxidant (e.g. Geyer et al., 2003; Brown et al., 2011). During nighttime winter RONOCO flights the total rate of reaction of NO₃ with alkenes was much reduced, but the rate of reaction of O₃ with alkenes was similar to that in summer. During day and night in winter, O₃ + alkene reactions were faster than NO₃ + alkene reactions. Overall, during RONOCO, the combined rate of alkene oxidation by O₃ and NO₃ was highest at night during summer.

Calculation of rates of instantaneous production of HO₂ from reactions of O₃ and NO₃ with alkenes, using measurements made during the flights, has revealed that nighttime production was dominated by NO₃ in summer and by O₃ in winter. The rate of instantaneous production of HO₂ from reactions of NO₃ with alkenes decreased significantly from summer to winter (87 %), whereas production from O₃ + alkene reactions was similar in summer and winter, decreasing by just 31 %. Strong positive correlation between HO₂ and NO₃, especially during flight B537, is attributed to the production of HO₂ from reactions of NO₃ with alkenes, particularly *trans*-2-butene and other isomers of butene.

Significant concentrations of HO₂ were detected at night, with the highest HO₂ concentration (13.6 pptv) being measured during a summer nighttime flight, indicating that HO_x radical chemistry remains active at night under the right conditions. The role of HO_x is diminished in the low photolysis winter daytime atmosphere, with alkene ozonolysis being primarily responsible for oxidation and radical initiation, in agreement with previous studies (e.g. Heard et al., 2004; Emmerson et al., 2005). Both the analysis presented here and the results of the box modelling study by Stone et al. (2014b) indicate that in air masses removed from sources of NO, NO₃ plays an important role in the oxidation of alkenes and radical initiation at night, in agreement with previous studies (e.g. Brown et al., 2011). Alkene ozonolysis also plays a significant role in nocturnal oxidation in agreement with Salisbury et al. (2001), Geyer et al. (2003), Ren et al. (2006), and others. The balance between the roles of NO₃ and O₃ was controlled

References

- Andrés-Hernández, M. D., Kartal, D., Crowley, J. N., Sinha, V., Regelin, E., Martínez-Harder, M., Nenakhov, V., Williams, J., Harder, H., Bozem, H., Song, W., Thieser, J., Tang, M. J., Hosaynali Beigi, Z., and Burrows, J. P.: Diel peroxy radicals in a semi-industrial coastal area: nighttime formation of free radicals, *Atmos. Chem. Phys.*, 13, 5731–5749, doi:10.5194/acp-13-5731-2013, 2013.
- Atkinson, R. and Arey, J.: Gas-phase tropospheric chemistry of biogenic volatile organic compounds: a review, *Atmos. Environ.*, 37, 197–219, 2003.
- Beames, J. M., Liu, F., Lu, L., and Lester, M. I.: Ultraviolet spectrum and photochemistry of the simplest Criegee intermediate CH_2OO , *J. Am. Chem. Soc.*, 134, 20045–20048, 2012.
- Beames, J. M., Liu, F., Lu, L., and Lester, M. I.: UV spectroscopic characterization of an alkyl substituted Criegee intermediate CH_3CHOO , *J. Chem. Phys.*, 138, 244307 doi:10.1063/1.4810865, 2013.
- Berndt, T. and Böge, O.: Kinetics of oxirane formation in the reaction of nitrate radicals with tetramethylethylene, *Ber. Bunsen Phys. Chem.*, 98, 869–871, 1994.
- Bey, I., Aumont, B., and Toupance, G.: A modeling study of the nighttime radical chemistry in the lower continental troposphere, *J. Geophys. Res.-Atmos.*, 106, 9991–10001, 2001.
- Bloss, C., Wagner, V., Bonzanini, A., Jenkin, M. E., Wirtz, K., Martin-Reviejo, M., and Pilling, M. J.: Evaluation of detailed aromatic mechanisms (MCMv3 and MCMv3.1) against environmental chamber data, *Atmos. Chem. Phys.*, 5, 623–639, doi:10.5194/acp-5-623-2005, 2005.
- Brown, S. S. and Stutz, J.: Nighttime radical observations and chemistry, *Chem. Soc. Rev.*, 41, 6405–6447, 2012.
- Brown, S. S., Dibb, J. E., Stark, H., Aldener, M., Vozella, M., Whitlow, S., Williams, E. J., Lerner, B. M., Jakoubek, R., Middlebrook, A. M., DeGouw, J. A., Warneke, C., Goldan, P. D., Kuster, W. C., Angevine, W. M., Sueper, D. T., Quinn, P. K., Bates, T. S., Meagher, J. F., Fehsenfeld, F. C., and Ravishankara, A. R.: Nighttime removal of NO_x in the summer marine boundary layer, *Geophys. Res. Lett.*, 31, L07108–L07113, 2004.
- Brown, S. S., Osthoff, H. D., Stark, H., Dubé, W. P., Ryerson, T. B., Warneke, C., de Gouw, J. A., Wollny, A. G., Parrish, D. D., Fehsenfeld, F. C., Ravishankara, A. R.: Aircraft observations of daytime NO_3 and N_2O_5 and their implications for tropospheric chemistry, *J. Photoch. Photobio. A*, 176, 270–278, 2005.

Nighttime measurements of HO_x during the RONOCO project

H. M. Walker et al.

Title Page

Abstract

Introduction

Conclusions

References

Tables

Figures



Back

Close

Full Screen / Esc

Printer-friendly Version

Interactive Discussion



**Nighttime
measurements of
HO_x during the
RONOCO project**

H. M. Walker et al.

Title Page

Abstract

Introduction

Conclusions

References

Tables

Figures



Back

Close

Full Screen / Esc

Printer-friendly Version

Interactive Discussion



- Donahue, N. M., Kroll, J. H., Anderson, J. G., and Demerjian, K. L.: Direct observation of OH production from the ozonolysis of olefins, *Geophys. Res. Lett.*, 25, 59–62, 1998.
- Donahue, N. M., Drozd, G. T., Epstein, S. A., Presto, A. A., and Kroll, J. H.: Adventures in ozoneland: down the rabbit-hole, *Phys. Chem. Chem. Phys.*, 13, 10848–10857, 2011.
- 5 Drozd, G. T. and Donahue, N. M.: Pressure dependence of stabilized Criegee intermediate formation from a sequence of alkenes, *J. Phys. Chem. A*, 115, 4381–4387, 2011.
- Dusanter, S., Vimal, D., Stevens, P. S., Volkamer, R., and Molina, L. T.: Measurements of OH and HO₂ concentrations during the MCMA-2006 field campaign – Part 1: Deployment of the Indiana University laser-induced fluorescence instrument, *Atmos. Chem. Phys.*, 9, 1665–1685, doi:10.5194/acp-9-1665-2009, 2009.
- 10 Edwards, G. D., Cantrell, C., Stephens, S., Hill, B., Goyea, O., Shetter, R., Mauldin, R. L., Kosciuch, E., Tanner, D., and Eisele, F.: Chemical ionization mass spectrometer instrument for the measurement of tropospheric HO₂ and RO₂, *Anal. Chem.*, 75, 5317–5327, 2003.
- Emmerson, K. M. and Carslaw, N.: Night-time radical chemistry during the TORCH campaign, *Atmos. Environ.*, 43, 3220–3226, 2009.
- 15 Emmerson, K. M. and Evans, M. J.: Comparison of tropospheric gas-phase chemistry schemes for use within global models, *Atmos. Chem. Phys.*, 9, 1831–1845, doi:10.5194/acp-9-1831-2009, 2009.
- Emmerson, K. M., Carslaw, N., and Pilling, M. J.: Urban atmospheric chemistry during the PUMA campaign 2: radical budgets for OH, HO₂ and RO₂, *J. Atmos. Chem.*, 52, 165–183, 2005.
- 20 Emmerson, K. M., Carslaw, N., Carslaw, D. C., Lee, J. D., McFiggans, G., Bloss, W. J., Gravestock, T., Heard, D. E., Hopkins, J., Ingham, T., Pilling, M. J., Smith, S. C., Jacob, M., and Monks, P. S.: Free radical modelling studies during the UK TORCH Campaign in Summer 2003, *Atmos. Chem. Phys.*, 7, 167–181, doi:10.5194/acp-7-167-2007, 2007.
- 25 Faloon, I. C., Tan, D., Leshner, R. L., Hazen, N. L., Frame, C. L., Simpas, J. B., Harder, H., Martinez, M., di Carlo, P., Ren, X., and Brune, W. H.: A laser-induced fluorescence instrument for detecting tropospheric OH and HO₂: characteristics and calibration, *J. Atmos. Chem.*, 47, 139–167, 2004.
- 30 Fleming, Z. L., Monks, P. S., Rickard, A. R., Heard, D. E., Bloss, W. J., Seakins, P. W., Still, T. J., Sommariva, R., Pilling, M. J., Morgan, R., Green, T. J., Brough, N., Mills, G. P., Penkett, S. A., Lewis, A. C., Lee, J. D., Saiz-Lopez, A., and Plane, J. M. C.: Peroxy radical chemistry and the

**Nighttime
measurements of
HO_x during the
RONOCO project**

H. M. Walker et al.

[Title Page](#)[Abstract](#)[Introduction](#)[Conclusions](#)[References](#)[Tables](#)[Figures](#)[Back](#)[Close](#)[Full Screen / Esc](#)[Printer-friendly Version](#)[Interactive Discussion](#)

control of ozone photochemistry at Mace Head, Ireland during the summer of 2002, *Atmos. Chem. Phys.*, 6, 2193–2214, doi:10.5194/acp-6-2193-2006, 2006.

Floquet, C. F. A.: Airborne Measurements of Hydroxyl Radicals by Fluorescence Assay by Gas Expansion, Ph.D. thesis, School of Chemistry, University of Leeds, Leeds, 155 pp., 2006.

Fuchs, H., Bohn, B., Hofzumahaus, A., Holland, F., Lu, K. D., Nehr, S., Rohrer, F., and Wahner, A.: Detection of HO₂ by laser-induced fluorescence: calibration and interferences from RO₂ radicals, *Atmos. Meas. Tech.*, 4, 1209–1225, doi:10.5194/amt-4-1209-2011, 2011.

Gerbig, C., Schmitgen, S., Kley, D., and Volz-Thomas, A.: An improved fast-response vacuum-UV resonance fluorescence CO instrument, *J. Geophys. Res.-Atmos.*, 104, 1699–1704, 1999.

German, K. R.: Direct measurement of the radiative lifetimes of the A²Σ⁺ (V' = 0), *J. Chem. Phys.*, 62, 2584–2587, 1975.

Geyer, A. and Stutz, J.: The vertical structure of OH-HO₂-RO₂ chemistry in the nocturnal boundary layer: a one-dimensional model study, *J. Geophys. Res.-Atmos.*, 109, D16301–D16316, 2004a.

Geyer, A. and Stutz, J.: Vertical profiles of NO₃, N₂O₅, O₃, and NO_x in the nocturnal boundary layer: 2. Model studies on the altitude dependence of composition and chemistry, *J. Geophys. Res.-Atmos.*, 109, D12307, doi:10.1029/2003JD004211, 2004b.

Geyer, A., Bächmann, K., Hofzumahaus, A., Holland, F., Konrad, S., Klüpfel, T., Pätz, H.-W., Perner, D., Mihelcic, D., Schäfer, H.-J., Volz-Thomas, A., and Platt, U.: Nighttime formation of peroxy and hydroxyl radicals during the BERLIOZ campaign: observations and modeling studies, *J. Geophys. Res.-Atmos.*, 108, 8249–8263, 2003.

Harrison, R. M., Yin, J., Tilling, R. M., Cai, X., Seakins, P. W., Hopkins, J. R., Lansley, D. L., Lewis, A. C., Hunter, M. C., Heard, D. E., Carpenter, L. J., Creasey, D. J., Lee, J. D., Pilling, M. J., Carslaw, N., Emmerson, K. M., Redington, A., Derwent, R. G., Ryall, D., Mills, G., and Penkett, S. A.: Measurement and modelling of air pollution and atmospheric chemistry in the U. K. West Midlands conurbation: overview of the PUMA consortium project, *Sci. Total Environ.*, 360, 5–25, 2006.

Heard, D. E.: Atmospheric field measurements of the hydroxyl radical using laser-induced fluorescence spectroscopy, *Annu. Rev. Phys. Chem.*, 57, 191–216, 2006.

Heard, D. E., Carpenter, L. J., Creasey, D. J., Hopkins, J. R., Lee, J. D., Lewis, A. C., Pilling, M. J., Seakins, P. W., Carslaw, N., and Emmerson, K. M.: High levels of the hy-

droxyl radical in the winter urban troposphere, *Geophys. Res. Lett.*, 31, L18112–L18117, doi:10.1029/2004gl020544, 2004.

Hewitt, C. N., Lee, J. D., MacKenzie, A. R., Barkley, M. P., Carslaw, N., Carver, G. D., Chappell, N. A., Coe, H., Collier, C., Commane, R., Davies, F., Davison, B., DiCarlo, P., Di Marco, C. F., Dorsey, J. R., Edwards, P. M., Evans, M. J., Fowler, D., Furneaux, K. L., Gallagher, M., Guenther, A., Heard, D. E., Helfter, C., Hopkins, J., Ingham, T., Irwin, M., Jones, C., Karunaharan, A., Langford, B., Lewis, A. C., Lim, S. F., MacDonald, S. M., Mahajan, A. S., Malpass, S., McFiggans, G., Mills, G., Misztal, P., Moller, S., Monks, P. S., Nemitz, E., Nicolas-Perea, V., Oetjen, H., Oram, D. E., Palmer, P. I., Phillips, G. J., Pike, R., Plane, J. M. C., Pugh, T., Pyle, J. A., Reeves, C. E., Robinson, N. H., Stewart, D., Stone, D., Whalley, L. K., and Yin, X.: Overview: oxidant and particle photochemical processes above a south-east Asian tropical rainforest (the OP3 project): introduction, rationale, location characteristics and tools, *Atmos. Chem. Phys.*, 10, 169–199, doi:10.5194/acp-10-169-2010, 2010.

Holland, F., Hofzumahaus, A., Schäfer, J., Kraus, A., and Pätz, H.-W.: Measurements of OH and HO₂ radical concentrations and photolysis frequencies during BERLIOZ, *J. Geophys. Res.-Atmos.*, 108, 8246–8261, 2003.

Hopkins, J. R., Lewis, A. C., and Read, K. A.: A two-column method for long-term monitoring of non-methane hydrocarbons (NMHCs) and oxygenated volatile organic compounds (*o*-VOCs), *J. Environ. Monitor.*, 5, 8–13, 2003.

Jenkin, M. E., Saunders, S. M., and Pilling, M. J.: The tropospheric degradation of volatile organic compounds: a protocol for mechanism development, *Atmos. Environ.*, 31, 81–104, 1997.

Jenkin, M. E., Saunders, S. M., Wagner, V., and Pilling, M. J.: Protocol for the development of the Master Chemical Mechanism, MCM v3 (Part B): tropospheric degradation of aromatic volatile organic compounds, *Atmos. Chem. Phys.*, 3, 181–193, doi:10.5194/acp-3-181-2003, 2003.

Johnson, D. and Marston, G.: The gas-phase ozonolysis of unsaturated volatile organic compounds in the troposphere, *Chem. Soc. Rev.*, 37, 699–716, 2008.

Jones, A. R., Thomson, D. J., Hort, M., and Devenish, B.: The UK Met Office's next-generation atmospheric dispersion model, NAME III, in: *Air Pollution Modeling and its Application XVII*, Proceedings of the 27th NATO/CCMS International Technical Meeting on Air Pollution Mod-

Nighttime measurements of HO_x during the RONOCO project

H. M. Walker et al.

Title Page

Abstract

Introduction

Conclusions

References

Tables

Figures



Back

Close

Full Screen / Esc

Printer-friendly Version

Interactive Discussion



**Nighttime
measurements of
HO_x during the
RONOCO project**

H. M. Walker et al.

Title Page

Abstract

Introduction

Conclusions

References

Tables

Figures



Back

Close

Full Screen / Esc

Printer-friendly Version

Interactive Discussion



elling and its Application, edited by: Borrego, C. and Norman, A.-L., Springer, Dordrecht, Netherlands, 580–589, 2007.

Kanaya, Y., Sadanaga, Y., Matsumoto, J., Sharma, U. K., Hirokawa, J., Kajii, Y., and Akimoto, H.: Nighttime observation of the HO₂ radical by an LIF instrument at Oki Island, Japan, and its possible origins, *Geophys. Res. Lett.*, 26, 2179–2182, 1999.

Kennedy, O. J., Ouyang, B., Langridge, J. M., Daniels, M. J. S., Bauguitte, S., Freshwater, R., McLeod, M. W., Ironmonger, C., Sendall, J., Norris, O., Nightingale, R., Ball, S. M., and Jones, R. L.: An aircraft based three channel broadband cavity enhanced absorption spectrometer for simultaneous measurements of NO₃, N₂O₅ and NO₂, *Atmos. Meas. Tech.*, 4, 1759–1776, doi:10.5194/amt-4-1759-2011, 2011.

Kroll, J. H., Clarke, J. S., Donahue, N. M., Anderson, J. G., and Demerjian, K. L.: Mechanism of HO_x formation in the gas-phase ozone-alkene reaction. 1. Direct, pressure-dependent measurements of prompt OH yields, *J. Phys. Chem. A*, 105, 1554–1560, 2001a.

Kroll, J. H., Sahay, S. R., Anderson, J. G., Demerjian, K. L., and Donahue, N. M.: Mechanism of HO_x formation in the gas-phase ozone-alkene reaction. 2. Prompt vs. thermal dissociation of carbonyl oxides to form OH, *J. Phys. Chem.-USA*, 105, 4446–4457, 2001b.

Kroll, J. H., Donahue, N. M., Cee, V. J., Demerjian, K. L., and Anderson, J. G.: Gas-phase ozonolysis of alkenes: formation of OH from anti carbonyl oxides, *J. Am. Chem. Soc.*, 124, 8518–8519, 2002.

Lee, J. D., Lewis, A. C., Monks, P. S., Jacob, M., Hamilton, J. F., Hopkins, J. R., Watson, N. M., Saxton, J. E., Ennis, C., Carpenter, L. J., Carslaw, N., Fleming, Z. L., Bandy, A., Oram, D. E., Penkett, S. A., Slemr, J., Norton, E. G., Rickard, A. R., Whalley, L. K., Heard, D. E., Bloss, W. J., Gravesstock, T., Smith, S. C., Stanton, J., Pilling, M. J., and Jenkin, M. E.: Ozone photochemistry and elevated isoprene during the UK heatwave of August 2003, *Atmos. Environ.*, 40, 7598–7613, 2006.

Lidster, R. T., Hamilton, J. F., Lee, J. D., Lewis, A. C., Hopkins, J. R., Punjabi, S., Rickard, A. R., and Young, J. C.: The impact of monoaromatic hydrocarbons on OH reactivity in the coastal UK boundary layer and free troposphere, *Atmos. Chem. Phys.*, 14, 6677–6693, doi:10.5194/acp-14-6677-2014, 2014.

Lightfoot, P. D., Cox, R. A., Crowley, J. N., Destriau, M., Hayman, G. D., Jenkin, M. E., Moortgat, G. K., and Zabel, F.: Organic peroxy radicals: kinetics, spectroscopy and tropospheric chemistry, *Atmos. Environ.*, 26A, 1805–1961, 1992.

**Nighttime
measurements of
HO_x during the
RONOCO project**

H. M. Walker et al.

Title Page

Abstract

Introduction

Conclusions

References

Tables

Figures



Back

Close

Full Screen / Esc

Printer-friendly Version

Interactive Discussion

- Lou, S., Holland, F., Rohrer, F., Lu, K., Bohn, B., Brauers, T., Chang, C.C., Fuchs, H., Häsel, R., Kita, K., Kondo, Y., Li, X., Shao, M., Zeng, L., Wahner, A., Zhang, Y., Wang, W., and Hofzumahaus, A.: Atmospheric OH reactivities in the Pearl River Delta – China in summer 2006: measurement and model results, *Atmos. Chem. Phys.*, 10, 11243–11260, doi:10.5194/acp-10-11243-2010, 2010.
- Lu, K. D., Rohrer, F., Holland, F., Fuchs, H., Bohn, B., Brauers, T., Chang, C. C., Häsel, R., Hu, M., Kita, K., Kondo, Y., Li, X., Lou, S. R., Nehr, S., Shao, M., Zeng, L. M., Wahner, A., Zhang, Y. H., and Hofzumahaus, A.: Observation and modelling of OH and HO₂ concentrations in the Pearl River Delta 2006: a missing OH source in a VOC rich atmosphere, *Atmos. Chem. Phys.*, 12, 1541–1569, doi:10.5194/acp-12-1541-2012, 2012.
- Lu, K. D., Hofzumahaus, A., Holland, F., Bohn, B., Brauers, T., Fuchs, H., Hu, M., Häsel, R., Kita, K., Kondo, Y., Li, X., Lou, S. R., Oebel, A., Shao, M., Zeng, L. M., Wahner, A., Zhu, T., Zhang, Y. H., and Rohrer, F.: Missing OH source in a suburban environment near Beijing: observed and modelled OH and HO₂ concentrations in summer 2006, *Atmos. Chem. Phys.*, 13, 1057–1080, doi:10.5194/acp-13-1057-2013, 2013.
- Lu, K. D., Rohrer, F., Holland, F., Fuchs, H., Brauers, T., Oebel, A., Dlugi, R., Hu, M., Li, X., Lou, S. R., Shao, M., Zhu, T., Wahner, A., Zhang, Y. H., and Hofzumahaus, A.: Nighttime observation and chemistry of HO_x in the Pearl River Delta and Beijing in summer 2006, *Atmos. Chem. Phys.*, 14, 4979–4999, doi:10.5194/acp-14-4979-2014, 2014.
- Martinez, M., Harder, H., Kubistin, D., Rudolf, M., Bozem, H., Eerdeken, G., Fischer, H., Klüpfel, T., Gurk, C., Königstedt, R., Parchatka, U., Schiller, C. L., Stickler, A., Williams, J., and Lelieveld, J.: Hydroxyl radicals in the tropical troposphere over the Suriname rainforest: airborne measurements, *Atmos. Chem. Phys.*, 10, 3759–3773, doi:10.5194/acp-10-3759-2010, 2010.
- Mauldin III, R. L., Berndt, T., Sipilä, M., Paasonen, P., Petäjä, T., Kim, S., Kurtén, A., Stratmann, F., Kerminen, V.-M., and Kulmala, M.: A new atmospherically relevant oxidant of sulphur dioxide, *Nature*, 488, 193–196, 2012.
- Morgan, W. T., Ouyang, B., Allan, J. D., Aruffo, E., Di Carlo, P., Kennedy, O. J., Lowe, D., Flynn, M. J., Rosenberg, P. D., Williams, P. I., Jones, R., McFiggans, G. B., and Coe, H.: Influence of aerosol chemical composition on N₂O₅ uptake: airborne regional measurements in North-Western Europe, *Atmos. Chem. Phys. Discuss.*, 14, 19673–19718, doi:10.5194/acpd-14-19673-2014, 2014.

**Nighttime
measurements of
HO_x during the
RONOCO project**

H. M. Walker et al.

Title Page

Abstract

Introduction

Conclusions

References

Tables

Figures



Back

Close

Full Screen / Esc

Printer-friendly Version

Interactive Discussion



- Nakajima, M. and Endo, Y.: Determination of the molecular structure of the simplest Criegee intermediate CH₂OO, *J. Chem. Phys.*, 139, 101103, doi:10.1063/1.4821165, 2013.
- Nakajima, M. and Endo, Y.: Spectroscopic characterization of an alkyl substituted Criegee intermediate *syn*-CH₃CHOO through pure rotational transitions, *J. Chem. Phys.*, 140, 011101, doi:10.1063/1.4861494, 2014.
- Ouyang, B., McLeod, M. W., Jones, R. L., and Bloss, W. J.: NO₃ radical production from the reaction between the Criegee intermediate CH₂OO and NO₂, *Phys. Chem. Chem. Phys.*, 15, 17070–17075, 2013.
- Paulson, S. E. and Orlando, J. J.: The reactions of ozone with alkenes: an important source of HO_x in the boundary layer, *Geophys. Res. Lett.*, 23, 3727–3730, 1996.
- Ren, X., Harder, H., Martinez, M., Leshner, R., Oligier, A., Simpasa, J. B., Brune, W. H., Schwab, J. J., Demerjian, K. L., He, Y., Zhou, X., and Gao, H.: OH and HO₂ chemistry in the urban atmosphere of New York City, *Atmos. Environ.*, 37, 3639–3651, 2003a.
- Ren, X., Harder, H., Martinez, M., Leshner, R. L., Oligier, A., Shirley, T., Adams, J., Simpasa, J. B., and Brune, W. H.: HO_x concentrations and OH reactivity observations in New York City during PMTACS-NY2001, *Atmos. Environ.*, 37, 3627–3637, 2003b.
- Ren, X., Brune, W. H., Mao, J., Mitchell, M. J., Leshner, R., Simpasa, J. B., Metcalf, A. R., Schwab, J. J., Cai, C., Li, Y., Demerjian, K. L., Felton, H. D., Boynton, G., Adams, A., Perry, J., He, Y., Zhou, X., and Hou, J.: Behavior of OH and HO₂ in the winter atmosphere in New York City, *Atmos. Environ.*, 40, 252–263, 2006.
- Salisbury, G., Rickard, A. R., Monks, P. S., Allan, B. J., Bauguitte, S. J. B., Penkett, S. A., Carslaw, N., Lewis, A. C., Creasey, D. J., Heard, D. E., Jacobs, P. J., and Lee, J. D.: Production of peroxy radicals at night via reactions of ozone and the nitrate radical in the marine boundary layer, *J. Geophys. Res.-Atmos.*, 106, 12669–12687, 2001.
- Saunders, S. M., Jenkin, M. E., Derwent, R. G., and Pilling, M. J.: Protocol for the development of the Master Chemical Mechanism, MCM v3 (Part A): tropospheric degradation of non-aromatic volatile organic compounds, *Atmos. Chem. Phys.*, 3, 161–180, doi:10.5194/acp-3-161-2003, 2003.
- Sheehy, P. M., Volkamer, R., Molina, L. T., and Molina, M. J.: Oxidative capacity of the Mexico City atmosphere – Part 2: A RO_x radical cycling perspective, *Atmos. Chem. Phys.*, 10, 6993–7008, doi:10.5194/acp-10-6993-2010, 2010.
- Shirley, T. R., Brune, W. H., Ren, X., Mao, J., Leshner, R., Cardenas, B., Volkamer, R., Molina, L. T., Molina, M. J., Lamb, B., Velasco, E., Jobson, T., and Alexander, M.: Atmo-

**Nighttime
measurements of
HO_x during the
RONOCO project**

H. M. Walker et al.

Title Page

Abstract

Introduction

Conclusions

References

Tables

Figures



Back

Close

Full Screen / Esc

Printer-friendly Version

Interactive Discussion



spheric oxidation in the Mexico City Metropolitan Area (MCMA) during April 2003, *Atmos. Chem. Phys.*, 6, 2753–2765, doi:10.5194/acp-6-2753-2006, 2006.

Smith, S. C., Lee, J. D., Bloss, W. J., Johnson, G. P., Ingham, T., and Heard, D. E.: Concentrations of OH and HO₂ radicals during NAMBLEX: measurements and steady state analysis, *Atmos. Chem. Phys.*, 6, 1435–1453, doi:10.5194/acp-6-1435-2006, 2006.

Sommariva, R., Pilling, M. J., Bloss, W. J., Heard, D. E., Lee, J. D., Fleming, Z. L., Monks, P. S., Plane, J. M. C., Saiz-Lopez, A., Ball, S. M., Bitter, M., Jones, R. L., Brough, N., Penkett, S. A., Hopkins, J. R., Lewis, A. C., and Read, K. A.: Night-time radical chemistry during the NAMBLEX campaign, *Atmos. Chem. Phys.*, 7, 587–598, doi:10.5194/acp-7-587-2007, 2007.

Sommariva, R., Osthoff, H. D., Brown, S. S., Bates, T. S., Baynard, T., Coffman, D., de Gouw, J. A., Goldan, P. D., Kuster, W. C., Lerner, B. M., Stark, H., Warneke, C., Williams, E. J., Fehsenfeld, F. C., Ravishankara, A. R., and Trainer, M.: Radicals in the marine boundary layer during NEAQS 2004: a model study of day-time and night-time sources and sinks, *Atmos. Chem. Phys.*, 9, 3075–3093, doi:10.5194/acp-9-3075-2009, 2009.

Stewart, D. J., Taylor, C. M., Reeves, C. E., and McQuaid, J. B.: Biogenic nitrogen oxide emissions from soils: impact on NO_x and ozone over west Africa during AMMA (African Monsoon Multidisciplinary Analysis): observational study, *Atmos. Chem. Phys.*, 8, 2285–2297, doi:10.5194/acp-8-2285-2008, 2008.

Still, T. J., Al-Haider, S., Seakins, P. W., Sommariva, R., Stanton, J. C., Mills, G., and Penkett, S. A.: Ambient formaldehyde measurements made at a remote marine boundary layer site during the NAMBLEX campaign – a comparison of data from chromatographic and modified Hantzsch techniques, *Atmos. Chem. Phys.*, 6, 2711–2726, doi:10.5194/acp-6-2711-2006, 2006.

Stone, D., Evans, M. J., Commane, R., Ingham, T., Floquet, C. F. A., McQuaid, J. B., Brookes, D. M., Monks, P. S., Purvis, R., Hamilton, J. F., Hopkins, J., Lee, J., Lewis, A. C., Stewart, D., Murphy, J. G., Mills, G., Oram, D., Reeves, C. E., and Heard, D. E.: HO_x observations over West Africa during AMMA: impact of isoprene and NO_x, *Atmos. Chem. Phys.*, 10, 9415–9429, doi:10.5194/acp-10-9415-2010, 2010.

Stone, D., Whalley, L. K., and Heard, D. E.: Tropospheric OH and HO₂ radicals: field measurements and model comparisons, *Chem. Soc. Rev.*, 41, 6348–6404, 2012.

Stone, D., Blitz, M., Daubney, L., Howes, N. U. M., and Seakins, P.: Kinetics of CH₂OO reactions with SO₂, NO₂, NO, H₂O and CH₃CHO as a function of pressure, *Phys. Chem. Chem. Phys.*, 16, 1139–1149, 2014a.

**Nighttime
measurements of
HO_x during the
RONOCO project**

H. M. Walker et al.

Title Page

Abstract

Introduction

Conclusions

References

Tables

Figures



Back

Close

Full Screen / Esc

Printer-friendly Version

Interactive Discussion

- Stone, D., Evans, M. J., Walker, H., Ingham, T., Vaughan, S., Ouyang, B., Kennedy, O. J., McLeod, M. W., Jones, R. L., Hopkins, J., Punjabi, S., Lidster, R., Hamilton, J. F., Lee, J. D., Lewis, A. C., Carpenter, L. J., Forster, G., Oram, D. E., Reeves, C. E., Bauguitte, S., Morgan, W., Coe, H., Aruffo, E., Dari-Salisburgo, C., Giammaria, F., Di Carlo, P., and Heard, D. E.: Radical chemistry at night: comparisons between observed and modelled HO_x, NO₃ and N₂O₅ during the RONOCO project, *Atmos. Chem. Phys.*, 14, 1299–1321, doi:10.5194/acp-14-1299-2014, 2014b.
- Stutz, J., Alicke, B., Ackermann, R., Geyer, A., White, A., and Williams, E.: Vertical profiles of NO₃, N₂O₅, O₃, and NO_x in the nocturnal boundary layer: 1. Observations during the Texas Air Quality Study 2000, *J. Geophys. Res.-Atmos.*, 109, D12306–D12320, 2004.
- Su, Y.-T., Huang, Y.-H., Witek, H. A., and Lee, Y.-P.: Infrared absorption spectrum of the simplest Criegee intermediate CH₂OO, *Science*, 340, 174–176, 2013.
- Taatjes, C. A., Meloni, G., Selby, T. M., Trevitt, A. J., Osborn, D. L., Percival, C. J., and Shallcross, D. E.: Direct observation of the gas-phase Criegee intermediate (CH₂OO), *J. Am. Chem. Soc.*, 130, 11883–11885, 2008.
- Taatjes, C. A., Welz, O., Eskola, A. J., Savee, J. D., Osborn, D. L., Lee, E. P. F., Dyke, J. M., Mok, D. W. K., Shallcross, D. E., and Percival, C. J.: Direct measurement of Criegee intermediate (CH₂OO) reactions with acetone, acetaldehyde, and hexafluoroacetone, *Phys. Chem. Chem. Phys.*, 14, 10391–10400, 2012.
- Taatjes, C. A., Welz, O., Eskola, A. J., Savee, J. D., Scheer, A. M., Shallcross, D. E., Rotavera, B., Lee, E. P. F., Dyke, J. M., Mok, D. W. K., Osborn, D. L., and Percival, C. J.: Direct measurements of conformer-dependent reactivity of the Criegee intermediate CH₃CHOO, *Science*, 340, 177–180, 2013.
- Taatjes, C. A., Shallcross, D. E., and Percival, C. J.: Research frontiers in the chemistry of Criegee intermediates and tropospheric ozonolysis, *Phys. Chem. Chem. Phys.*, 16, 1689–2180, 2014.
- Vereecken, L. and Francisco, J. S.: Theoretical studies of atmospheric reaction mechanisms in the troposphere, *Chem. Soc. Rev.*, 41, 6217–6708, 2012.
- Volkamer, R., Sheehy, P., Molina, L. T., and Molina, M. J.: Oxidative capacity of the Mexico City atmosphere – Part 1: A radical source perspective, *Atmos. Chem. Phys.*, 10, 6969–6991, doi:10.5194/acp-10-6969-2010, 2010.

**Nighttime
measurements of
HO_x during the
RONOCO project**

H. M. Walker et al.

Title Page

Abstract

Introduction

Conclusions

References

Tables

Figures

◀

▶

◀

▶

Back

Close

Full Screen / Esc

Printer-friendly Version

Interactive Discussion



Welz, O., Savee, J. D., Osborn, D. L., Vasu, S. S., Percival, C. J., Shallcross, D. E., and Taatjes, C. A.: Direct kinetic measurements of Criegee intermediate (CH₂OO) formed by reaction of CH₂I with O₂, *Science*, 335, 204–207, 2012.

Whalley, L. K., Furneaux, K. L., Goddard, A., Lee, J. D., Mahajan, A., Oetjen, H., Read, K. A., Kaaden, N., Carpenter, L. J., Lewis, A. C., Plane, J. M. C., Saltzman, E. S., Wiedensohler, A., and Heard, D. E.: The chemistry of OH and HO₂ radicals in the boundary layer over the tropical Atlantic Ocean, *Atmos. Chem. Phys.*, 10, 1555–1576, doi:10.5194/acp-10-1555-2010, 2010.

Whalley, L. K., Blitz, M. A., Desservettaz, M., Seakins, P. W., and Heard, D. E.: Reporting the sensitivity of laser-induced fluorescence instruments used for HO₂ detection to an interference from RO₂ radicals and introducing a novel approach that enables HO₂ and certain RO₂ types to be selectively measured, *Atmos. Meas. Tech.*, 6, 3425–3440, doi:10.5194/amt-6-3425-2013, 2013.

Winiberg, F. A. F., Smith, S. C., Bejan, I., Brumby, C. A., Ingham, T., Malkin, T. L., Orr, S. C., Heard, D. E., and Seakins, P. W.: Pressure dependent calibration of the OH and HO_x channels of a FAGE HO_x instrument using the Highly Instrumented Reactor for Atmospheric Chemistry (HIRAC), *Atmos. Meas. Tech. Discuss.*, 7, 7963–8011, doi:10.5194/amtd-7-7963-2014, 2014.

Wong, K. W. and Stutz, J.: Influence of nocturnal vertical stability on daytime chemistry: a one-dimensional model study, *Atmos. Environ.*, 44, 3753–3760, 2010.

Nighttime measurements of HO_x during the RONOCO project

H. M. Walker et al.

[Title Page](#)
[Abstract](#)
[Introduction](#)
[Conclusions](#)
[References](#)
[Tables](#)
[Figures](#)
[Back](#)
[Close](#)
[Full Screen / Esc](#)
[Printer-friendly Version](#)
[Interactive Discussion](#)


Table 1. Examples of modelling studies and observations of HO_x radicals and VOC oxidation at night. PERCA = Peroxy Radical Chemical Amplification; LIF = Laser Induced Fluorescence; DOAS = Differential Optical Absorption Spectroscopy; MCM = Master Chemical Mechanism; MIESR = Matrix Isolation Electron Spin Resonance; RACM = Regional Atmospheric Chemistry Mechanism; CRDS = Cavity Ring Down Spectroscopy; CIMS = Chemical Ionisation Mass Spectrometry; GC = Gas Chromatography; PTRMS = Proton Transfer Reaction Mass Spectrometry; FTIR = Fourier Transform Infrared Spectroscopy; DUALER (DUAL channel peroxy radical chemical amplifier); OA-CRD = Off Axis Cavity Ring Down Spectroscopy; CRM-PTR-MS = Comparative Reactivity Method Proton Transfer Mass Spectrometry.

Location, Campaign, Date	Methods	Results	Reference
Mace Head, Ireland, EASE97, 1997	Measurements: [HO ₂ + RO ₂] measured by PERCA; HO _x measured by LIF; NO ₃ measured by DOAS. Modelling: Campaign-tailored box model constrained to measurements, based on MCM.	2 nights of HO _x measurements: HO ₂ = 1–2 and 0.5–0.7 pptv; OH not detected above limit of detection (~2.5 × 10 ⁵ cm ⁻³). NO ₃ dominated radical production in westerly (clean) air masses; O ₃ dominated in NE, SE, and SW air masses and dominated radical production overall during the campaign.	Salisbury et al. (2001); Creasey et al. (2002)
Pabstthum, Germany, BERLIOZ 1998,	Measurements: HO _x measured by LIF; NO ₃ measured by DOAS and MIESR. Modelling: Zero-dimensional model using lumped VOC reactivity, constrained to measured species.	Nighttime OH = 1.85 × 10 ⁵ cm ⁻³ , compared to modelled value of 4.1 × 10 ⁵ cm ⁻³ . Nighttime HO ₂ = 3 × 10 ⁷ cm ⁻³ , model results in agreement. NO ₃ chemistry responsible for 53 % of HO ₂ and 36 % of OH during the night. O ₃ + alkenes responsible for 47 % of HO ₂ and 64 % of OH during the night.	Geyer et al. (2003); Holland et al. (2003)
Birmingham, PUMA, 1999 and 2000	Measurements: HO _x measured by LIF. Modelling: Photochemical box model constrained to measurements, based on MCM.	Daytime OH initiation dominated by O ₃ + alkenes, HONO photolysis, and O(¹ D) + H ₂ O during summer. O ₃ + alkenes dominated in winter. O ₃ + alkenes main radical source at night.	Emmerson et al. (2005); Harrison et al. (2006)
New York, PMTACS-NY, 2001	Measurements: HO _x measured by LIF.	Nighttime OH ~ 7 × 10 ⁵ cm ⁻³ and nighttime HO ₂ ~ 8 × 10 ⁵ cm ⁻³ . Increase in HO _x after midnight attributed to increase in O ₃ due to transport. O ₃ + alkenes main source of nighttime HO _x .	Ren et al. (2003a, b)
Mace Head, NAMBLEX, 2002	Measurements: HO _x measured by LIF; NO ₃ measured by DOAS. Modelling: Zero-dimensional box models constrained to measured species, based on MCM.	Nighttime HO ₂ = 2–3 × 10 ⁷ cm ⁻³ ; OH below detection limit (6 × 10 ⁴ cm ⁻³). Model overestimated HO ₂ . On average, O ₃ + alkene reactions contributed 59 % and NO ₃ + alkene reactions contributed 41 % to RO ₂ production at night, but NO ₃ and RO ₂ concentrations were always higher in semi-polluted air masses than in clean marine air masses and NO ₃ reactions dominated in these conditions.	Fleming et al. (2006); Smith et al. (2006); Sommariva et al. (2007)

Nighttime measurements of HO_x during the RONOCO project

H. M. Walker et al.

Title Page

Abstract

Introduction

Conclusions

References

Tables

Figures



Back

Close

Full Screen / Esc

Printer-friendly Version

Interactive Discussion



Table 1. Continued.

Location, Campaign, Date	Methods	Results	Reference
Writtle, London, TORCH, 2003	Measurements: HO _x measured by LIF, RO ₂ measured by PERCA, during a heatwave/pollution episode. Modelling: zero-dimensional box model constrained to measured species.	OH and HO ₂ observed above the limit of detection on several nights. OH peaked at $8.5 \times 10^5 \text{ cm}^{-3}$; HO ₂ peaked at $1 \times 10^8 \text{ cm}^{-3}$. Model overpredicted nighttime OH and HO ₂ on average by 24 and 7%; underpredicted $[\text{HO}_2 + \sum \text{RO}_2]$ by 22%.	Lee et al. (2006); Emmerson et al. (2007); Emmerson and Carslaw (2009)
Mexico City, MCMA 2003	Measurements: HO _x measured by LIF, NO ₃ measured by DOAS. Modelling: Zero-dimensional model based on MCM v3.1, constrained to measured species.	Polluted city location characterized by high levels of NO, NO ₂ and O ₃ . Maximum nighttime OH $\sim 1 \times 10^6 \text{ cm}^{-3}$; maximum nighttime HO ₂ ~ 6 pptv. Night-time production of radicals dominated by O ₃ + alkene reactions (76–92%); NO ₃ + alkene plays a minor role. Daytime radical production $\sim 25\times$ higher than night.	Shirley et al. (2006); Sheehy et al. (2010); Volkamer et al. (2010)
New York City, PMTACS-NY winter 2004	Measurements: HO _x measured by LIF. Modelling: Zero-dimensional model based on RACM and constrained by measurements.	Mean maximum OH = 0.05 pptv; mean maximum HO ₂ = 0.7 pptv. Model underprediction of HO ₂ was pronounced when NO was high. O ₃ + alkene reactions were dominant nighttime source.	Ren et al. (2006)
Gulf of Maine, Northeast United States, NEAQS, 2004	Measurements: NO ₃ and N ₂ O ₅ measured by CRDS. Modelling: Zero-dimensional model based on MCM v3.1, constrained to measured species. No measurements of OH, HO ₂ , or RO ₂ .	Ship-based measurements onboard RV <i>Ronald H. Brown</i> in the Gulf of Maine, influenced by unpolluted marine air masses and polluted air masses from USA and Canada. Maximum modelled nighttime HO ₂ = $7.0 \times 10^8 \text{ cm}^{-3}$. Base model overestimated NO ₃ and NO ₂ observations by 30–50%. In anthropogenic air masses reaction with VOCs and RO ₂ each accounted for 40% of modelled NO ₃ loss.	Sommariva et al. (2009)
Houston, Texas, TexAQS, 2006	Measurements: NO ₃ and N ₂ O ₅ measured by CRDS, VOCs measured by CIMS, GC, and PTRMS. No direct measurements of OH, HO ₂ , or RO ₂ .	Loss rates and budgets of NO ₃ and highly reactive VOCs calculated. NO ₃ primarily lost through reaction with VOCs. VOC oxidation dominated by NO ₃ , which was 3–5 times more important than O ₃ .	Brown et al. (2011)

Nighttime measurements of HO_x during the RONOCO project

H. M. Walker et al.

Title Page

Abstract

Introduction

Conclusions

References

Tables

Figures

◀

▶

◀

▶

Back

Close

Full Screen / Esc

Printer-friendly Version

Interactive Discussion



Table 1. Continued.

Location, Campaign, Date	Methods	Results	Reference
Pearl River Delta, China, PRIDE-PRD, 2006	Measurements: HO _x measured by LIF; OH reactivity measured by laser-flash photolysis and LIF; VOCs measured by FTIR and GC. Modelling: Box model based on RACM and the Mainz Isoprene Mechanism, and constrained by measurements.	Rural site 60 km downwind of large urban region (Guangzhou), with low local wind speeds favouring accumulation of air pollutants. Maximum nighttime OH (hourly average) = $5 \times 10^6 \text{ cm}^{-3}$; maximum nighttime HO ₂ (hourly average) = $1 \times 10^9 \text{ cm}^{-3}$. Unknown recycling mechanism required for the model to reproduce measured nighttime values. OH reactivity peaked at night. Missing nighttime reactivity attributed to unmeasured secondary organic compounds.	Lou et al. (2010, 2012, 2013a)
Beijing, CAREBEI-JING2006, 2006	Measurements: HO _x measured by LIF; OH lifetime measured by laser flash photolysis and LIF; VOCs measured by GC. Modelling: Box model based on RACM and the Mainz Isoprene Mechanism, and constrained by measurements.	Suburban rural site south of Beijing, under the influence of slowly moving, aged polluted air from the south. OH reactivity peaked at night. Model generally underestimated observed nighttime OH concentrations.	Lu et al. (2013a, b)
Cape Verde, RHaMBLe, 2007	Measurements: HO _x measured by LIF. Modelling: Box model based on MCM with added halogen chemistry scheme, constrained to measurements of long-lived species.	Clean tropical Atlantic measurement site with occasional continental influence. OH was not measured at night. HO ₂ was detected on two nights, up to $2.5 \times 10^7 \text{ cm}^{-3}$. Model underprediction of HO ₂ was significantly reduced by constraining the model to 100 pptv of peroxy acetyl nitrate (PAN) at night.	Whalley et al. (2010)
Huelva, Spain, DOMINO, 2008	Measurements: [HO ₂ + RO ₂] measured by DUALER; HO _x measured by LIF; NO ₃ and N ₂ O ₅ measured by OA-CRD; OH reactivity measured by CRM-PTR-MS. No measurements of anthropogenic VOCs.	Coastal forested site with strong urban-industrial and weak biogenic influences. Maxima in [HO ₂ + RO ₂] and [HO ₂] were observed around noon and midnight. Enhanced nighttime [HO ₂ + RO ₂] (up to 80 pptv) was observed in air masses from the urban-industrial region. Maximum nighttime HO ₂ = 8 pptv. Measured NO ₃ was generally below LOD; calculated NO ₃ up to 20 pptv. Calculated production of RO ₂ from NO ₃ + alkenes accounts for 47–54% of observed [HO ₂ + RO ₂]. Ozonolysis of unmeasured alkenes could account for remaining [HO ₂ + RO ₂].	Andrés-Hernández et al. (2009)

Nighttime measurements of HO_x during the RONOCO project

H. M. Walker et al.

Title Page

Abstract

Introduction

Conclusions

References

Tables

Figures

◀

▶

◀

▶

Back

Close

Full Screen / Esc

Printer-friendly Version

Interactive Discussion



Table 2. Details of supporting measurements.

Species	Instrument, Technique	Time resolution; Limit of detection (LOD)	References
CO	Aero Laser AL5002 Fast Carbon Monoxide Monitor. Excitation and fast response fluorescence at $\lambda = 150$ nm.	1 s; 3.5 ppbv	Gerbig et al. (1999)
O ₃	Thermo Scientific TEi49C Ozone analyser. Absorption spectroscopy at $\lambda = 254$ nm.	1 s; 0.6 ppbv	Hewitt et al. (2010)
NO, NO ₂ , NO _x (NO + NO ₂)	Air Quality Design dual channel fast-response NO _x instrument. Chemiluminescence from NO + O ₃ reaction. Conversion of NO ₂ to NO by photolysis.	10 s; 3 pptv for NO, 15 pptv for NO ₂	Stewart et al. (2008)
NO ₂ , \sum ANs, \sum PN _s	TD-LIF (thermal dissociation laser induced fluorescence). Detection of NO ₂ by laser-induced fluorescence. Thermal decomposition of \sum ANs (total alkyl nitrate) and \sum PN _s (total peroxy nitrate) to NO ₂ .	1 s; 9.8 pptv for NO ₂ , 28.1 pptv for \sum ANs, 18.4 pptv for \sum PN _s	Dari-Salisburgo et al. (2009); Di Carlo et al. (2013)
Alkenes	Whole air samples (WAS) analysed by laboratory-based gas chromatography with flame ionization detection (GC-FID).	Typically 30 s; variable limits of detection	Hopkins et al. (2003)
NO ₃ , N ₂ O ₅	BBCEAS (broadband cavity-enhanced absorption spectroscopy) of NO ₃ at $\lambda = 642$ – 672 nm. N ₂ O ₅ measured following thermal dissociation to NO ₃ + NO ₂ .	1 s; 1.1 pptv for NO ₃ , 2.4 pptv for NO ₃ + N ₂ O ₅	Kennedy et al. (2011)
HCHO	Hantzsch technique: Liquid-phase reaction of formaldehyde followed by excitation, and fluorescence of resulting adduct at $\lambda = 510$ nm.	60 s; 81 pptv	Still et al. (2006)

Nighttime measurements of HO_x during the RONOCO project

H. M. Walker et al.

Table 3. Mean mixing ratios of selected gas phase species, and air temperature, measured during RONOCO and SeptEx. The flight and season during which the maximum values were measured are given in parentheses. NO₂ data are from the TD-LIF instrument. Zero values indicate measurements below the limit of detection.

Species	Summer RONOCO	SeptEx	Winter RONOCO	Maximum
CO/ppbv	102.3	117.1	139.3	256.0 (B537, summer)
O ₃ /ppbv	39.6	40.4	38.6	89.8 (B537, summer)
NO ₃ /pptv	21.1	0	6.2	176.9 (B537, summer)
NO/ppbv	0.05	0	0	18.9 (B539, summer)
NO ₂ /ppbv	1.6	1.7	2.3	18.6 (B568, winter)
Temperature/K	286.5	286.2	276.4	297.5 (B537, summer)

Title Page

Abstract

Introduction

Conclusions

References

Tables

Figures

◀

▶

◀

▶

Back

Close

Full Screen / Esc

Printer-friendly Version

Interactive Discussion



Nighttime measurements of HO_x during the RONOCO project

H. M. Walker et al.

Title Page

Abstract

Introduction

Conclusions

References

Tables

Figures

◀

▶

◀

▶

Back

Close

Full Screen / Esc

Printer-friendly Version

Interactive Discussion



Table 4. Combined daytime and nighttime mean concentrations of OH and mean mixing ratios of HO₂ with the FAGE instrument's average 1 σ limits of detection during the RONOCO and SeptEx fieldwork.

	OH/molecule cm ⁻³		HO ₂ /pptv	
	Mean concentration	Limit of detection	Mean mixing ratio	Limit of detection
Summer		1.8×10^6	1.6	0.03
SeptEx	1.8×10^6	1.2×10^6	2.9	0.02
Winter		6.4×10^5	0.7	0.02

Nighttime measurements of HO_x during the RONOCO project

H. M. Walker et al.

Title Page

Abstract

Introduction

Conclusions

References

Tables

Figures



Back

Close

Full Screen / Esc

Printer-friendly Version

Interactive Discussion



Table 5. Mean and, in parentheses, maximum HO₂ mixing ratios measured during RONOCO and SeptEx.

	Mean (maximum) HO ₂ mixing ratio/pptv		
	Summer	SeptEx	Winter
Dawn	0.74 (1.19)		0.54 (1.81)
Day		3.78 (11.79)	0.49 (1.68)
Dusk	2.73 (9.97)		0.32 (0.97)
Night	1.86 (13.58)		0.98 (2.02)

Nighttime
measurements of
HO_x during the
RONOCO project

H. M. Walker et al.

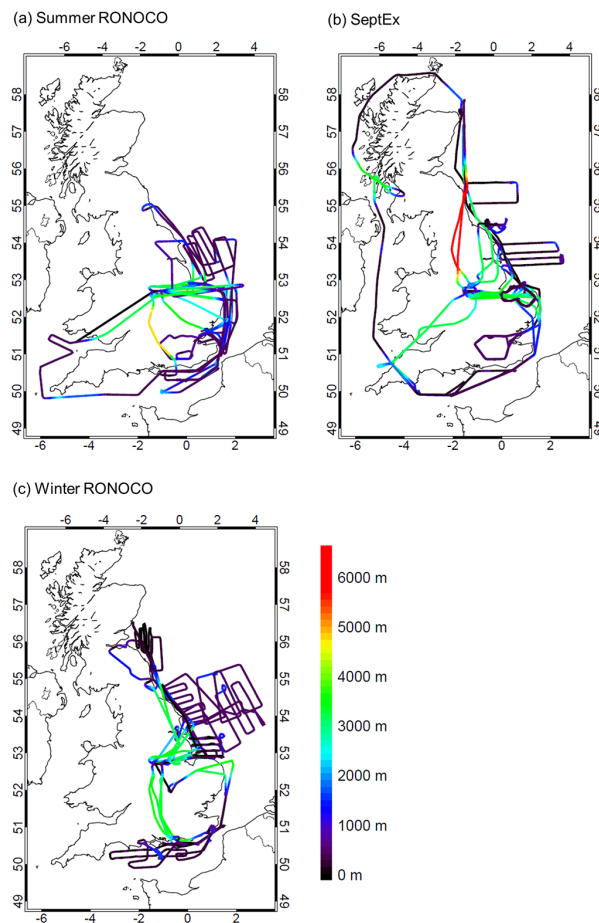


Figure 1. Flight paths for: **(a)** Summer RONOCO, **(b)** SeptEx, and **(c)** winter RONOCO measurement campaigns, coloured by altitude.

[Title Page](#)[Abstract](#)[Introduction](#)[Conclusions](#)[References](#)[Tables](#)[Figures](#)[◀](#)[▶](#)[◀](#)[▶](#)[Back](#)[Close](#)[Full Screen / Esc](#)[Printer-friendly Version](#)[Interactive Discussion](#)

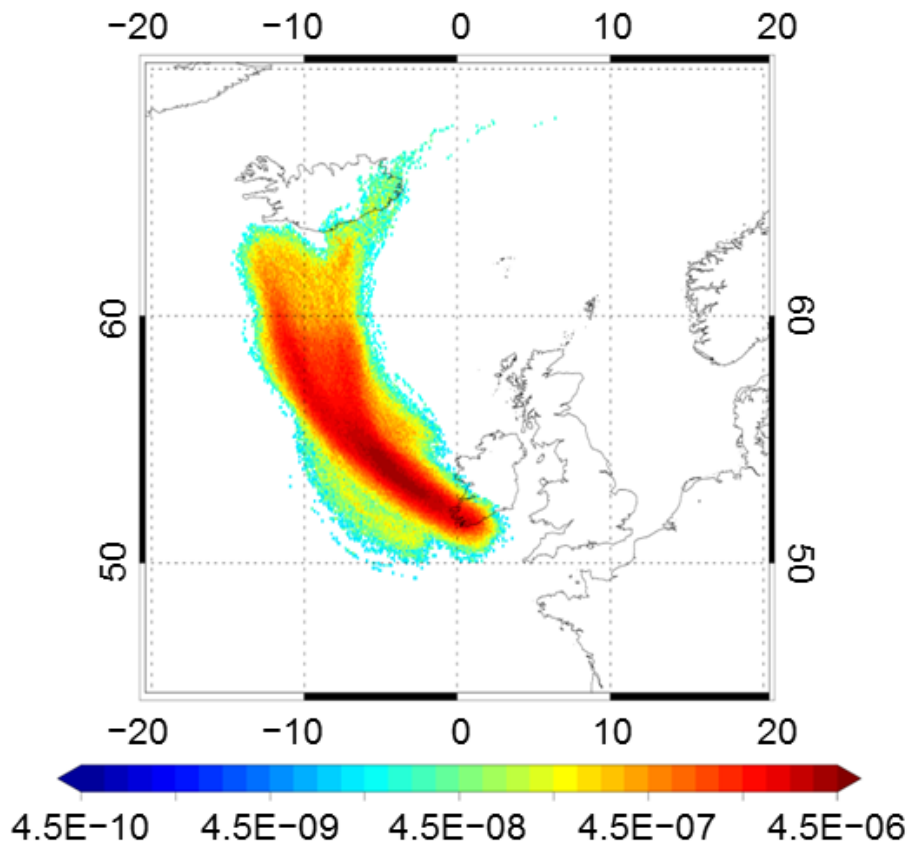


Figure 2. Footprint map for flight B535 on 17 July 2010, showing model particle densities (g m^{-3}) in a 300 m deep layer from the surface, integrated over a 24 h period beginning 48 h prior to the flight.

Nighttime measurements of HO_x during the RONOCO project

H. M. Walker et al.

Title Page

Abstract Introduction

Conclusions References

Tables Figures

◀ ▶

◀ ▶

Back Close

Full Screen / Esc

Printer-friendly Version

Interactive Discussion



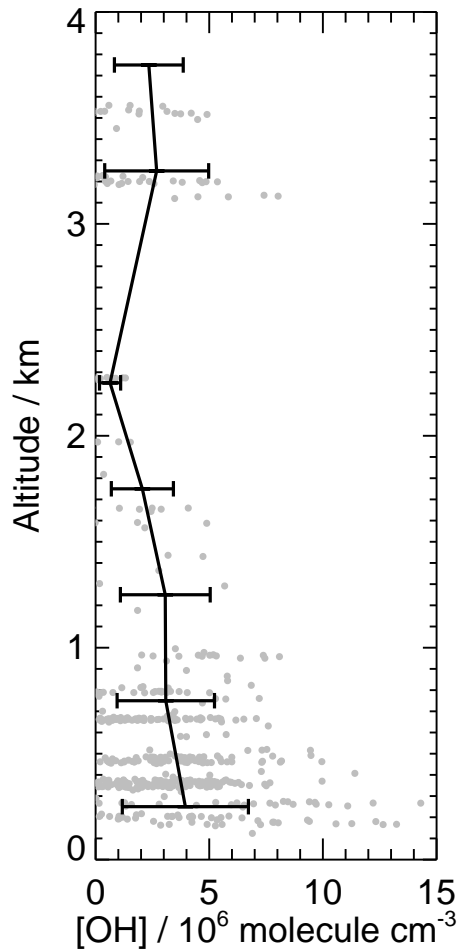


Figure 3. Altitude profile of OH measured during SeptEx showing 60 s data (grey points) and mean values in 500 m altitude bins (solid black lines). Error bars are 1σ .

Nighttime measurements of HO_x during the RONOCO project

H. M. Walker et al.

Title Page

Abstract Introduction

Conclusions References

Tables Figures

◀ ▶

◀ ▶

Back Close

Full Screen / Esc

Printer-friendly Version

Interactive Discussion



Nighttime
measurements of
HO_x during the
RONOCO project

H. M. Walker et al.

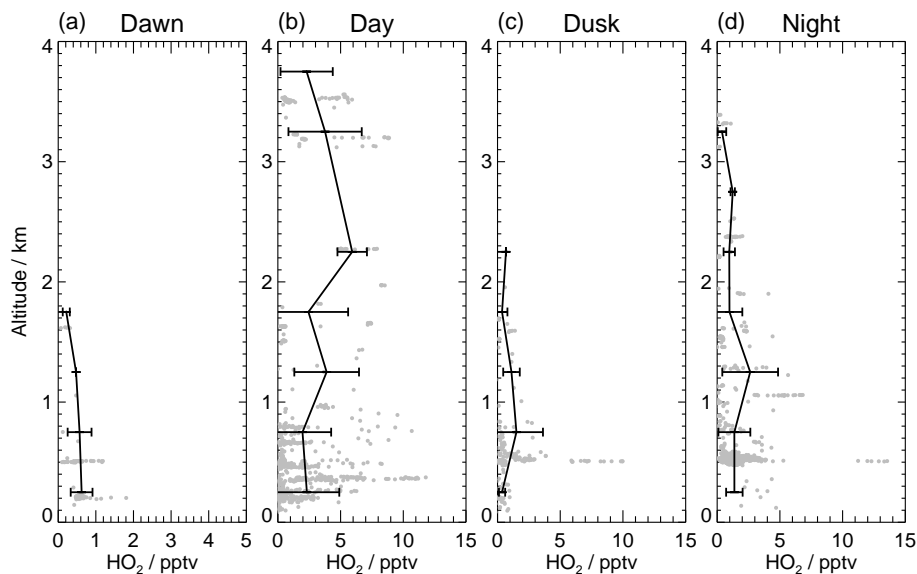


Figure 4. Altitude profiles of HO₂ measured in RONOCO and SeptEx during: **(a)** dawn; **(b)** day; **(c)** dusk; **(d)** night, showing 60 s data (grey points) and mean values in 500 m altitude bins (solid black lines). Error bars are 1σ.

[Title Page](#)[Abstract](#)[Introduction](#)[Conclusions](#)[References](#)[Tables](#)[Figures](#)[◀](#)[▶](#)[◀](#)[▶](#)[Back](#)[Close](#)[Full Screen / Esc](#)[Printer-friendly Version](#)[Interactive Discussion](#)

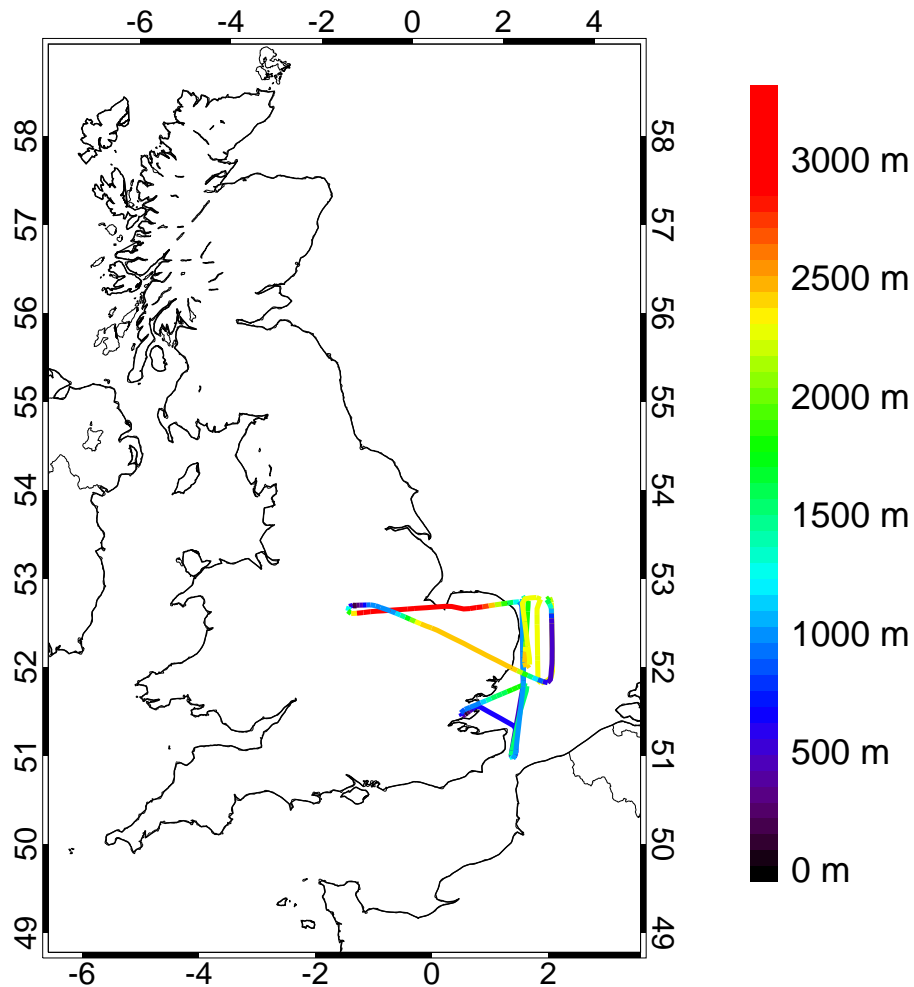


Figure 5. Flight track of flight B537 on 20 July 2010, coloured by altitude.

Nighttime measurements of HO_x during the RONOCO project

H. M. Walker et al.

Title Page

Abstract

Introduction

Conclusions

References

Tables

Figures

◀

▶

◀

▶

Back

Close

Full Screen / Esc

Printer-friendly Version

Interactive Discussion



Nighttime
measurements of
 HO_x during the
RONOCO project

H. M. Walker et al.

Title Page

Abstract

Introduction

Conclusions

References

Tables

Figures

◀

▶

◀

▶

Back

Close

Full Screen / Esc

Printer-friendly Version

Interactive Discussion

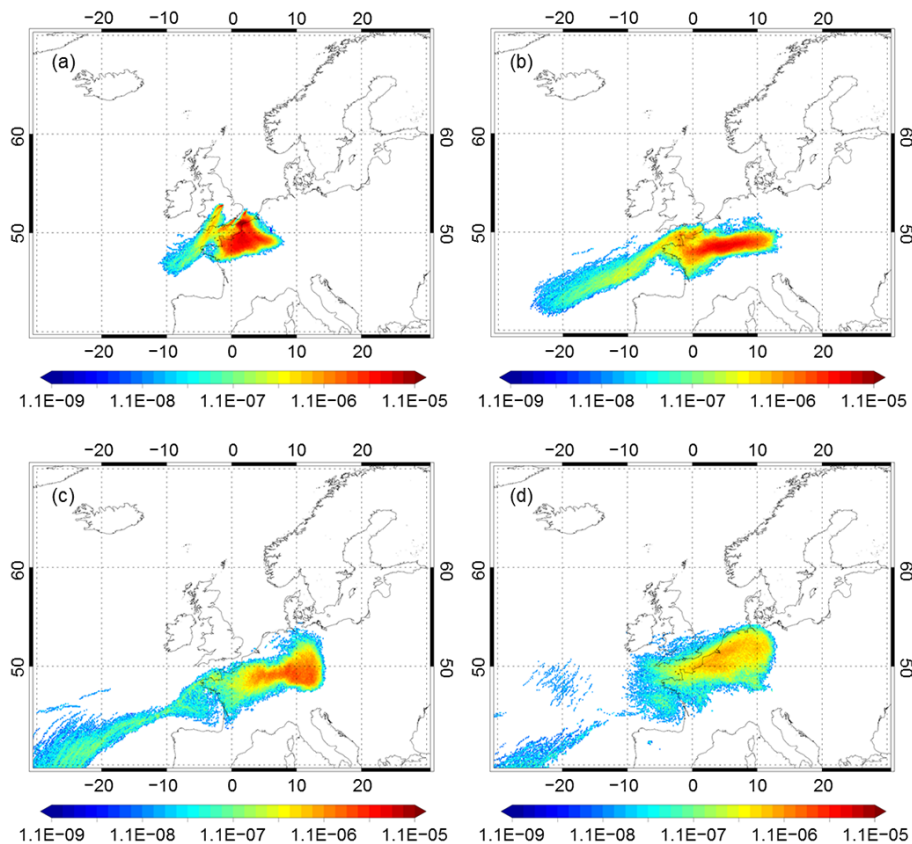


Figure 6. Footprint maps for flight B537 on 20 July 2010, showing model particle densities (g s^{-3}) in a 300 m deep layer from the surface, integrated over 24 h periods beginning (a) 24 h, (b) 48 h, (c) 72 h, and (d) 96 h prior to the flight.

Nighttime
measurements of
HO_x during the
RONOCO project

H. M. Walker et al.

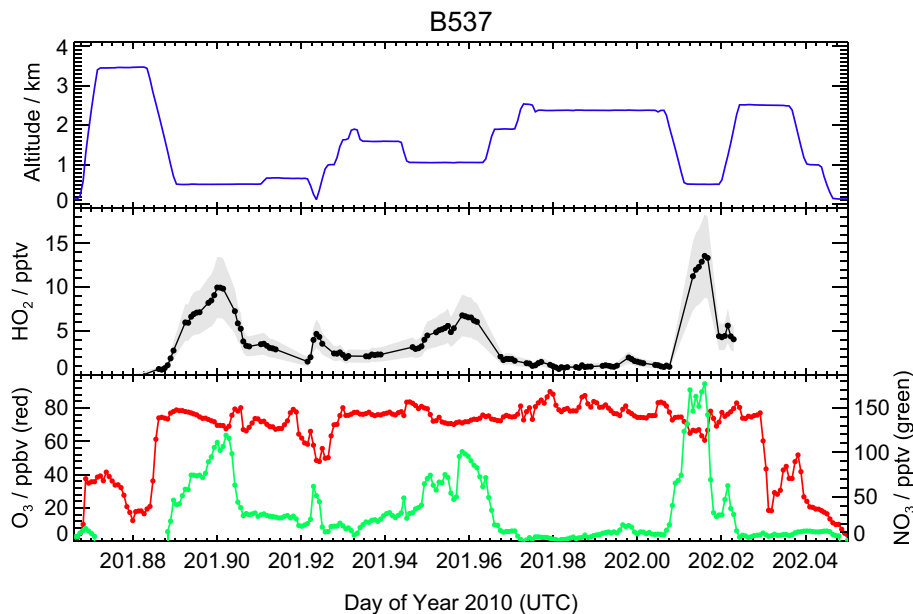


Figure 7. Time series of altitude (top panel, blue), HO₂ (middle panel, black, with grey shading representing the uncertainty in the measurements), O₃ (bottom panel, red) and NO₃ (bottom panel, green) during nighttime flight B537 on 20 July 2010.

[Title Page](#)[Abstract](#)[Introduction](#)[Conclusions](#)[References](#)[Tables](#)[Figures](#)[◀](#)[▶](#)[◀](#)[▶](#)[Back](#)[Close](#)[Full Screen / Esc](#)[Printer-friendly Version](#)[Interactive Discussion](#)

Nighttime
measurements of
HO_x during the
RONOCO project

H. M. Walker et al.

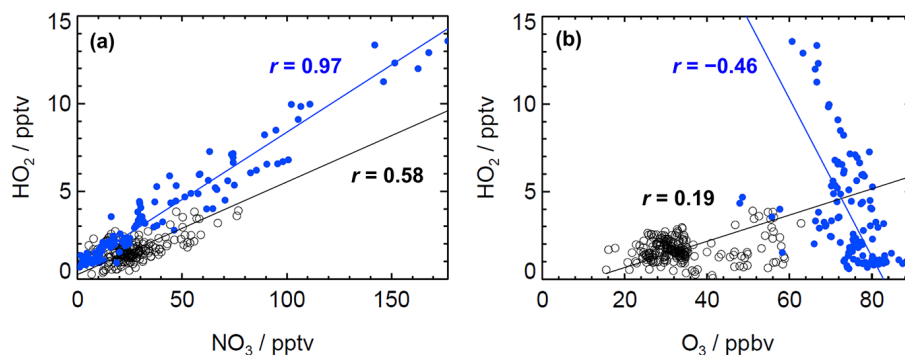


Figure 8. HO₂ vs. (a) NO₃ and (b) O₃ during flight B537 (blue, filled circles) and during all other nighttime flights (black, open circles). The solid lines are lines of best fit to the data.

[Title Page](#)[Abstract](#)[Introduction](#)[Conclusions](#)[References](#)[Tables](#)[Figures](#)[Back](#)[Close](#)[Full Screen / Esc](#)[Printer-friendly Version](#)[Interactive Discussion](#)

Nighttime measurements of HO_x during the RONOCO project

H. M. Walker et al.

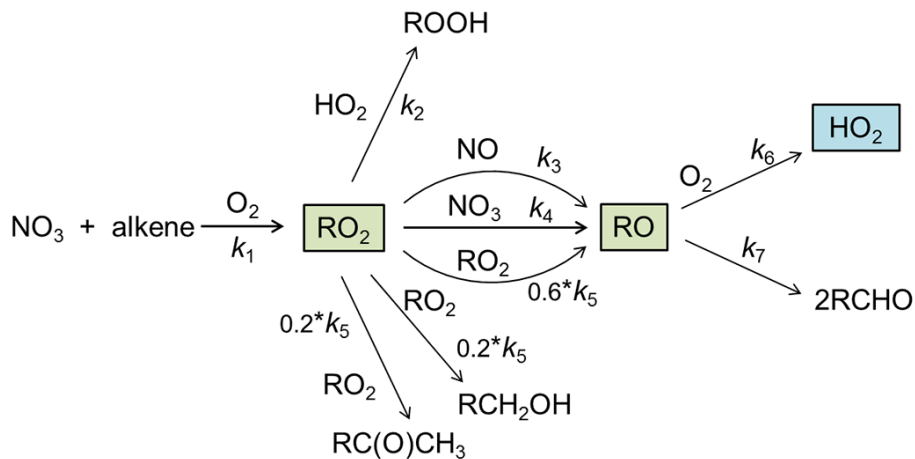


Figure 9. Generalised reaction scheme for production of RO_2 and HO_2 following reaction of NO_3 with an alkene.

Title Page

Abstract

Introduction

Conclusions

References

Tables

Figures



Back

Close

Full Screen / Esc

Printer-friendly Version

Interactive Discussion



Nighttime measurements of HO_x during the RONOCO project

H. M. Walker et al.

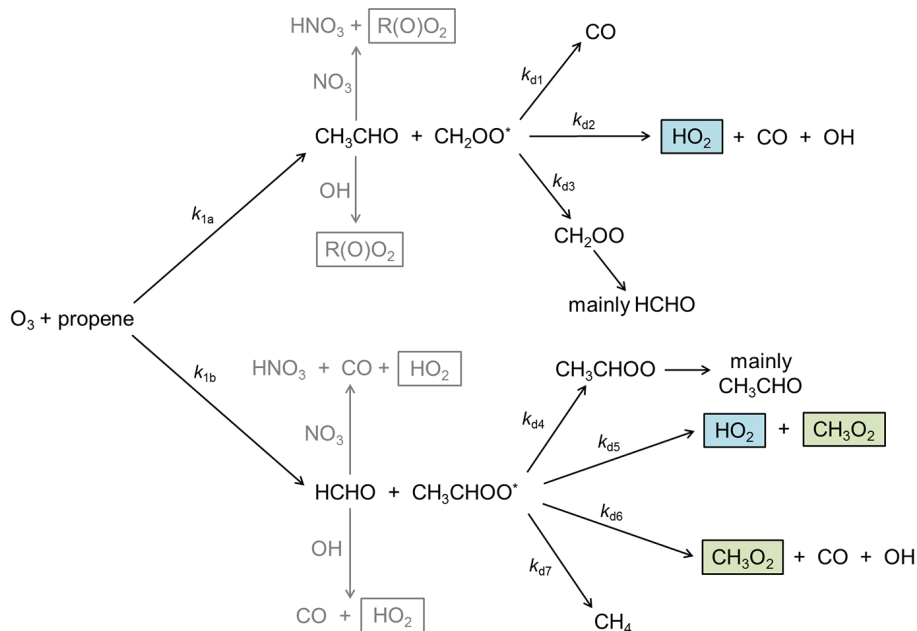


Figure 10. Reaction scheme for $O_3 + \text{propene}$, showing production of HO_2 and the methyl peroxy radical, CH_3O_2 .

Title Page

Abstract Introduction

Conclusions References

Tables Figures

◀ ▶

◀ ▶

Back Close

Full Screen / Esc

Printer-friendly Version

Interactive Discussion



Nighttime measurements of HO_x during the RONOCO project

H. M. Walker et al.

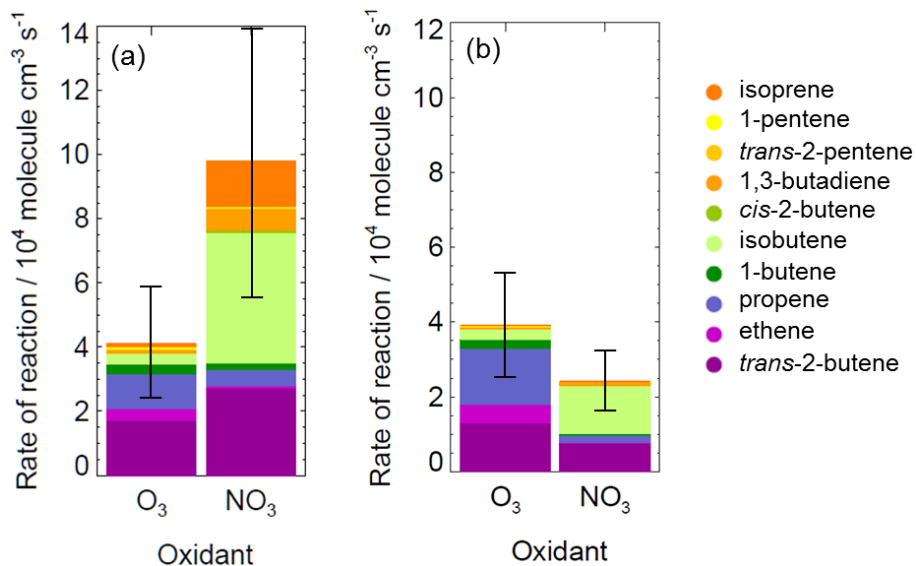


Figure 11. Nighttime rates of reaction between O₃ and NO₃ with alkenes during: **(a)** summer; and **(b)** winter RONOCO flights. Error bars represent the combined uncertainty in the measurements.

Nighttime measurements of HO_x during the RONOCO project

H. M. Walker et al.

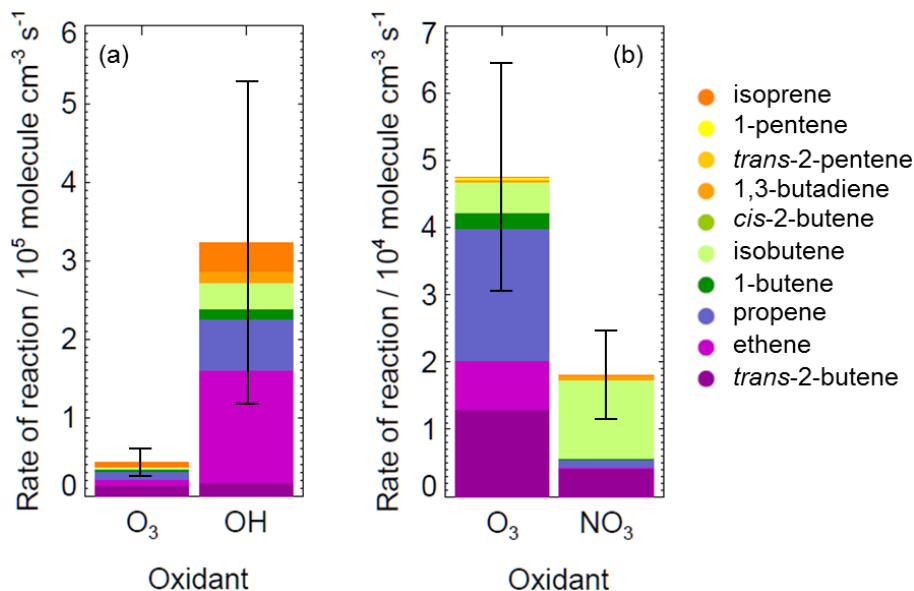


Figure 12. Daytime rates of reaction of (a) O₃ and OH with alkenes during SeptEx; and (b) O₃ and NO₃ with alkenes during winter. Note the different scales. NO₃ was not detected during daytime SeptEx flights (LOD = 1.1 pptv); OH was not detected during daytime winter flights (LOD = 6.4 × 10⁵ molecule cm⁻³). Error bars represent the combined uncertainties in the measurements.

Nighttime measurements of HO_x during the RONOCO project

H. M. Walker et al.

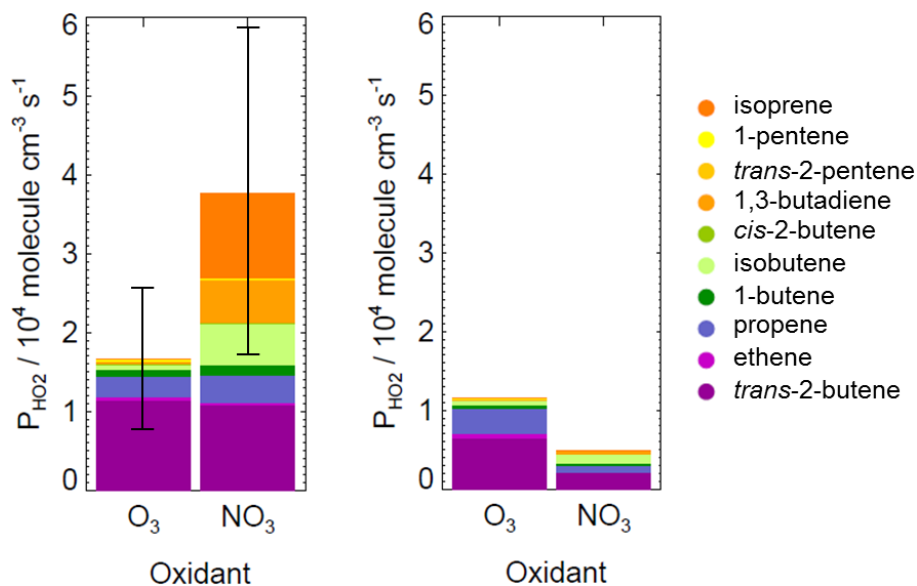


Figure 13. Averaged rates of instantaneous production of HO₂ from reactions of O₃ and NO₃ with alkenes during: **(a)** summer; and **(b)** winter RONOCO flights. Error bars represent the combined uncertainty in the measurements.

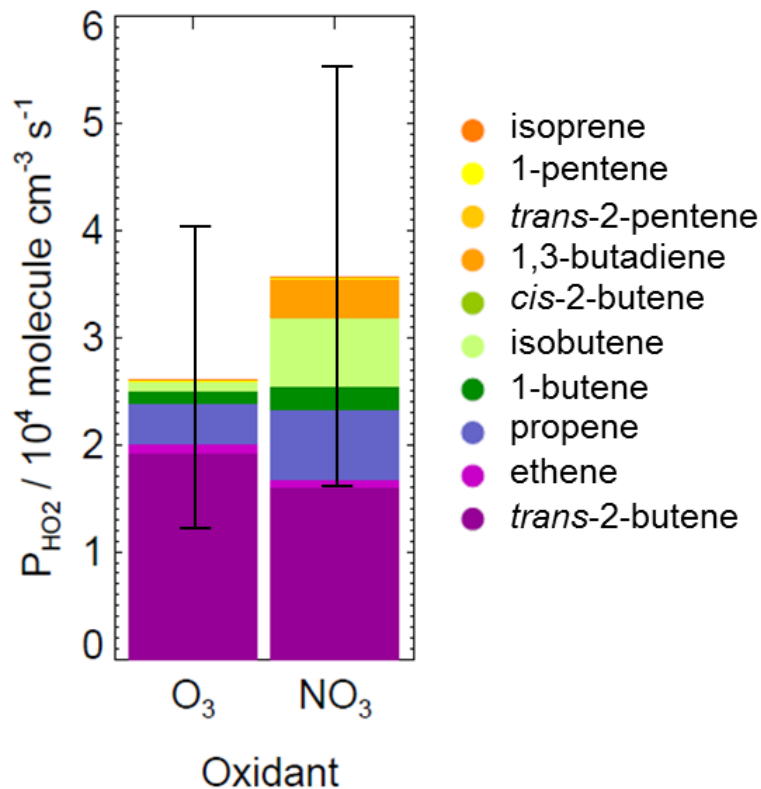


Figure 14. Rates of instantaneous production of HO₂ (P_{HO_2}) from reactions of O₃ and NO₃ with alkenes during flight B537. Error bars represent the combined uncertainty in the measurements.

